

FACTORIZATIONS OF DIFFEOMORPHISMS OF COMPACT SURFACES WITH BOUNDARY

ANDY WAND

ABSTRACT. We study diffeomorphisms of compact, oriented surfaces, developing methods of distinguishing those which have positive factorizations into Dehn twists from those which satisfy the weaker condition of right veering. We use these to construct open book decompositions of Stein-fillable 3-manifolds whose monodromies have no positive factorization.

1. INTRODUCTION

Let Σ be a compact, orientable surface with nonempty boundary. The (restricted) mapping class group of Σ , denoted Γ_Σ , is the group of isotopy classes of orientation preserving diffeomorphisms of Σ which restrict to the identity on $\partial\Sigma$. The goal of this paper is to study the monoid $Dehn^+(\Sigma, \partial\Sigma) \subset \Gamma_\Sigma$ of products of right Dehn twists. In particular, we are able to show:

Theorem 1.1. *There exist open book decompositions which support Stein fillable contact structures but whose monodromies cannot be factorized into positive Dehn twists.*

This result follows from much more general results which we develop concerning $Dehn^+(\Sigma, \partial\Sigma)$. We develop necessary conditions on the images of properly embedded arcs under these diffeomorphisms, and also necessary conditions for elements of the set of curves which can appear as twists in some positive factorization of a given $\varphi \in \Gamma_\Sigma$. The first of these can be thought of as a strengthening of the *right veering* condition, which dates at least as far back as Thurston's proof of the left orderability of the braid group, and which was introduced into the study of contact structures by Honda, Kazez, and Matic in [HKM]. In that paper, it is shown that the monoid $Veer(\Sigma, \partial\Sigma) \subset \Gamma_\Sigma$ of right-veering diffeomorphisms (see Section 2 for definitions) strictly contains $Dehn^+(\Sigma, \partial\Sigma)$. Our methods allow one to easily distinguish certain elements of $Veer(\Sigma, \partial\Sigma) \setminus Dehn^+(\Sigma, \partial\Sigma)$.

Central to much of current research is the relation between the monodromy of an open book decomposition and the fillability of the contact structure. The starting point is the remarkable theorem of Giroux [Gi], demonstrating a one-to-one correspondence between oriented contact structures on a 3-manifold M up to isotopy and open book decompositions of M up to positive stabilization. It has been shown by Giroux and by Loi and Peirgallini ([Gi], [LP]) that any open book with monodromy which can be factorized into positive Dehn twists supports a Stein-fillable contact structure, that every Stein fillable-structure is supported by *some* open book with factorization into positive twists, and in [HKM] that an open book's monodromy is right-veering if and only if the supported structure is tight. The question of whether *each* open book which supports a Stein fillable

structure must be positive, answered in the negative by our Theorem 1.1, has been a long-standing open question.

Section 2 introduces some conventions and definitions, and provides motivation for what is to come. Section 3 introduces the concept of a *right position* for the monodromy image of a properly embedded arc in Σ , and compatibility conditions for right positions on collections of arc images under a given monodromy. More importantly, we show that a monodromy can have a positive factorization only if the images of any collection of nonintersecting properly embedded arcs in Σ admit right positions which are pairwise compatible. We use this to construct simple examples of open books whose monodromies, though right veering (see Section 2 for a precise definition), have no positive factorization.

In Section 4 we use these results to address the question of under what conditions various isotopy classes of curves on a surface can be shown not to appear as Dehn twists in any positive factorization of a given monodromy, obtaining various necessary conditions under certain assumptions on the monodromy.

Finally, in Section 5, we construct explicit examples of open book decompositions which support Stein fillable contact structures yet whose monodromies have no positive factorizations. For the construction we demonstrate a method of modifying a certain mapping class group relation (the lantern relation) into an ‘immersed’ configuration, which we then use to modify certain open books with positively factored monodromies (which therefore support Stein fillable contact manifolds) into stabilization equivalent books (which support the same contact structures) whose monodromies now have non-trivial negative twisting. We then apply the methods developed in the previous sections to show that in fact this negative twisting is essential.

It has come to our attention that Baker, Etnyre, and Van Horn-Morris [BEV] have recently constructed similar examples of non-positive open books, all of which use the same surface, $\Sigma_{2,1}$, involved in our construction. Their argument for non-positivity, however, is specific to this surface, hinging on the non-triviality of the first homology group of the mapping class group of the surface (with its boundary capped off), which does not hold for surfaces of higher genus.

We would like to thank Danny Calegari for many helpful comments on a previous version of this paper, and Rob Kirby for his support and encouragement throughout the much extended period over which it was written.

2. PRELIMINARIES

Throughout, Σ denotes a compact, orientable surface with nonempty boundary. The (restricted) mapping class group of Σ , denoted Γ_Σ , is the group of isotopy classes of orientation preserving diffeomorphisms of Σ which restrict to the identity on $\partial\Sigma$. In general we will not distinguish between a diffeomorphism and its isotopy class.

Let $SCC(\Sigma)$ be the set of simple closed curves on Σ . For $\alpha \in SCC(\Sigma)$, cutting Σ along α , twisting one of the sides by 360 degrees to the right and gluing back gives a self-diffeomorphism of Σ , the *positive Dehn twist* about α , which we denote by τ_α . The inverse operation, τ_α^{-1} , is a *negative Dehn twist*. It can easily be seen that the mapping class of τ_α depends only on the isotopy class of α .

We call $\varphi \in \Gamma_\Sigma$ *positive* if it can be factored as a product of positive Dehn twists.

An open book decomposition (Σ, φ) , where $\varphi \in \Gamma_\Sigma$, for a 3-manifold M with binding K is a homeomorphism between $(\Sigma \times [0, 1]) / \sim_\varphi, (\partial\Sigma \times [0, 1]) / \sim_\varphi$ and (M, K) . The equivalence relation \sim_φ is generated by $(x, 0) \sim_\varphi (\varphi(x), 1)$ for $x \in \Sigma$ and $(y, t) \sim_\varphi (y, t')$ for $y \in \partial\Sigma$.

Definition 2.1. For a surface Σ and positive mapping class φ , we define the positive extension $p.e.(\varphi) \subset SCC(\Sigma)$ as the set of all $\alpha \in SCC(\Sigma)$ such that τ_α appears as a twist in some positive factorization of φ .

A recurring theme of this paper is to use properly embedded arcs $\gamma_i \hookrightarrow \Sigma$ to understand what conditions on $p.e.(\varphi)$ can be derived from the geometric information of the monodromy images $\varphi(\gamma_i)$ (relative to the arcs themselves). Our general method is as follows: Suppose that P is some property of pairs $(\varphi(\gamma), \gamma)$ (which we abbreviate by referring to P as a property of the image $\varphi(\gamma)$) which holds for the case φ is the identity, and is preserved by positive Dehn twists, and that P holds for a given $\varphi(\gamma)$. Suppose then that $\alpha \in p.e.(\varphi)$; then there is a positive factorization of φ in which τ_α is a twist. Using the well known braid relation, we can assume τ_α is the *final* twist, and so the monodromy given by $\tau_\alpha^{-1} \circ \varphi$ is also positive, and thus P holds for $(\tau_\alpha^{-1} \circ \varphi)(\gamma)$ as well.

As a motivating example, consider a pair of arcs $\gamma, \gamma' : [0, 1] \hookrightarrow \Sigma$ which share an endpoint $\gamma(0) = \gamma'(0) = x \in \partial\Sigma$, isotoped to minimize intersection. Following [HKM], we say γ' is ‘to the right’ of γ , denoted $\gamma' \geq \gamma$, if either the pair is isotopic, or if the tangent vectors $(\dot{\gamma}'(0), \dot{\gamma}(0))$ define the orientation of Σ at x . The property of being ‘to the right’ of γ (at x) is then a property of images $\varphi(\gamma)$ which satisfies the conditions of the previous paragraph, so we may conclude that, if $\varphi(\gamma)$ is to the right of γ , then $\alpha \in p.e.(\varphi)$ only if $(\tau_\alpha^{-1} \circ \varphi)(\gamma)$ is to the right of γ .

A closely related definition which will be made use of throughout the paper is the following (due again to Honda, Kazez and Matic in [HKM]):

Definition 2.2. Let φ be a positive mapping class in Γ_Σ , $\gamma \hookrightarrow \Sigma$ a properly embedded arc with endpoint $x \in \partial\Sigma$. Then φ is right veering if, for each such γ and x , the image $\varphi(\gamma)$ is to the right of γ at x .

Our aim in this paper is to determine conditions which must be satisfied by *pairs* of images in a positive factorization. As an initial step, we consider what it should mean for two arcs to have ‘the same’ images under φ . An obvious candidate is the following:

Definition 2.3. Let γ be a properly embedded arc in Σ , φ a right-veering monodromy. Define the step-down $\mathcal{C}_{\varphi(\gamma)}$ as the embedded multi-curve on Σ obtained by slicing $\varphi(\gamma)$ along γ , and re-attaching the endpoints as in Figure 1.

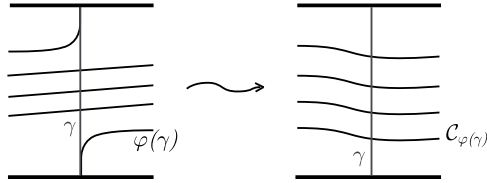


FIGURE 1. Construction of step-down

The stepdown thus allows us to relate distinct arcs to a common object, a multicurve. We want to say that a pair of arcs has in some sense ‘the same’ image if they have the same stepdown:

Definition 2.4. *Let γ_1, γ_2 be properly embedded arcs in Σ , and $\varphi \in \Gamma_\Sigma$. We say the pair γ_1, γ_2 is parallel under φ if $\mathcal{C}_{\varphi(\gamma_1)}$ is isotopic to $\mathcal{C}_{\varphi(\gamma_2)}$.*

As it stands, however, this condition is far too strict to be of any practical use. Our approach then is to ‘localize’ these ideas by decomposing the monodromy images of arcs into segments which we may then compare across distinct arc images. As we shall see in the following section, this approach allows one under certain circumstances to derive useful information concerning positivity of a given monodromy beyond that given by right veering, purely from the geometric information of its arc images.

3. RIGHT POSITION

In this section, we develop the idea of a *right position* for the monodromy image of a properly embedded arc in Σ , and develop consistency conditions which allow us to prove:

Theorem 3.1. *Let Σ be a compact surface with boundary, $\varphi \in \Gamma_\Sigma$ admit a positive factorization into Dehn twists, and $\{\gamma_i\}_{i=1}^n, n \geq 1$, be a collection of non-intersecting, properly embedded arcs in Σ . Then $\{(\gamma_i, \varphi(\gamma_i))\}_{i=1}^n$ admit consistent right positions.*

In particular, following the argument of the previous section, it follows that, for $\alpha \in SCC(\Sigma)$, $\alpha \in p.e.(\varphi)$ only if for each pair of arcs γ_1, γ_2 , the pairs $(\gamma_1, \tau_\alpha^{-1}(\varphi(\gamma_1))), (\gamma_2, \tau_\alpha^{-1}(\varphi(\gamma_2)))$ admit consistent right positions. As we shall see, this allows simple construction of examples of right veering monodromies with no positive factorization.

Definition 3.2. *Given a properly embedded arc $\gamma \hookrightarrow \Sigma$ with boundary $\{c, c'\}$, and $\varphi \in \Gamma_\Sigma$ right-veering, with $\varphi(\gamma), \gamma$ isotoped to minimize the number of connected components of $\gamma \cap \varphi(\gamma)$, let A be the set of positively oriented intersections in $\gamma \cap \varphi(\gamma)$ (sign conventions are illustrated in Figure 2). A right position $\mathcal{P} = \mathcal{P}(\varphi, \gamma)$ is a set of points $\{v_j\}_{j=0}^n$, where $v_0 = c, v_n = c'$, and $\{v_i\}_{i=1}^{n-1} \subset A$, such that no two points lie in the same connected component of A .*

Observation 3.3. *Note that we do not require the positively oriented intersections of $\gamma \cap \varphi(\gamma)$ to be a discrete set. In particular, they are not required to be transverse.*

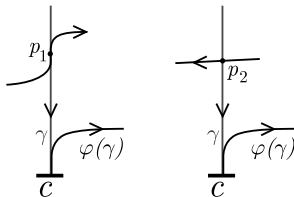


FIGURE 2. p_1 is a positive, p_2 a negative, point of $\gamma \cap \varphi(\gamma)$

Associated to a right position is the set $H(\mathcal{P}) := \{[v_i, v_j] \subset \varphi(\gamma) \mid v_i, v_j \in \mathcal{P}\}$. We denote these segments by $h_{i,j}$, or, if only a single endpoint is required, simply use h_i to denote a subarc starting from v_i and extending as long as the context requires, in which case direction of extension along $\varphi(\gamma)$ will be clear from context.

Right position can thus be thought of as a way of distinguishing ‘horizontal’ segments $H(\mathcal{P})$, separated by the ‘vertical’ points \mathcal{P} (Figure 3). Note that for any right-veering φ , and any properly embedded arc γ , $(\gamma, \varphi(\gamma))$ has a trivial right position consisting of the points $\partial(\gamma)$, and so there is a single horizontal segment $h_{0,1} = \varphi(\gamma)$. Furthermore, if A is nonempty, there is at least one non-trivial right position. Intuitively, the vertical points play a role analogous to the initial (boundary) points of the arc, allowing us to localize the global ‘right’ness of an arc image through the decomposition into horizontal segments (this will be made more precise further on in the paper).

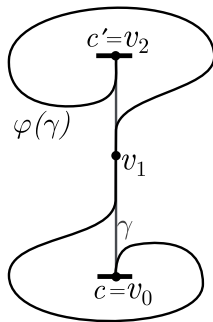


FIGURE 3. $\mathcal{P} = \{v_0, v_1, v_2\}$ is a right position of $\gamma, \varphi(\gamma)$. There are three distinct horizontal segments: $h_{0,1}, h_{1,2}$, and $h_{0,2}$

We are interested in using right position to compare *pairs* of arcs; the idea being that, if φ is positive, we expect to be able to view any pair of horizontal segments as either unrelated, or as belonging to the ‘same’ horizontal segment.

Throughout, when considering pairs $\mathcal{P}_1, \mathcal{P}_2$ of right positions, we use v and h for, respectively, vertical points and horizontal segments of \mathcal{P}_1 , w and g for \mathcal{P}_2 .

To get started, we need to be able to compare horizontal segments. To that end, we have:

Definition 3.4. *Let γ_1, γ_2 be distinct, properly embedded arcs in Σ , $\varphi \in \Gamma_\Sigma$, and $\mathcal{P}_i = \mathcal{P}_i(\varphi, \gamma_i)$ a right position for $i = 1, 2$. We say that $h_j \in H(\mathcal{P}_1), g_k \in H(\mathcal{P}_2)$ are initially parallel (along B) if there is an embedded disc $B \hookrightarrow \Sigma$ bounded by $\gamma_1, g_k, \gamma_2, h_j$, such that each of h_j, g_k lies to the left of the other (as viewed traveling along either arc away from the vertical point), on which v_j, w_k are corners. Alternately, if each of h_j, g_k is oriented away from the vertical point, then the orientations give an orientation of ∂B (see Figure 4).*

So, to say that a pair of horizontal segments is ‘unrelated’ is to say that they are not initially parallel. It is left to clarify what we expect of initially parallel segments h_j, g_k . The idea is to extend the notion of being parallel up to a second pair of vertical points v_l, w_m , and thus to the horizontal segments $h_{j,l}, g_{k,m}$, such that the pair is ‘completed’; i.e. h_l, g_m are themselves initially parallel in the opposite direction, and the embedded discs complete one another to form a ‘singular

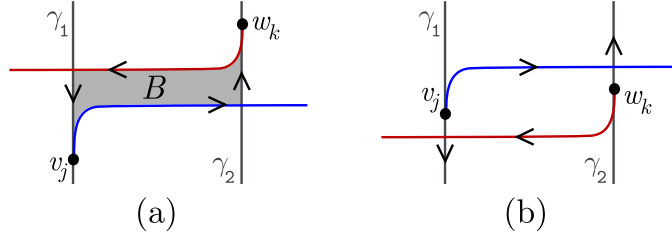


FIGURE 4. (a) h_j and g_k are initially parallel along B . (b) h_j and g_k are not initially parallel.

annulus' (Figure 5) (notice that there is no further restriction on intersections of the embedded discs, so that the 'singular annulus' is possibly immersed, rather than embedded). To be precise:

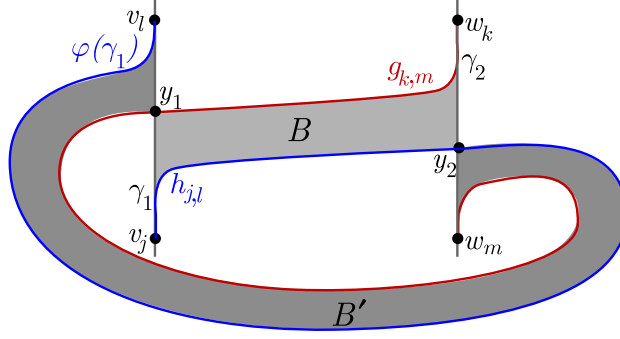


FIGURE 5. Horizontal segments $h_{j,l}, g_{k,m}$ complete one another, forming the boundary of a 'singular annulus'.

Definition 3.5. Let h_j, g_k be initially parallel along B , with corners v_j, w_k, y_1, y_2 , where $y_i \in \gamma_i$ for $i = 1, 2$. Then the pair h_j, g_k are completed if there are (unique) vertical points $v_l \in \mathcal{P}_1, w_m \in \mathcal{P}_2$, which we call the endpoints, such that the arcs $\gamma_1, \gamma_2, h_{j,l}, g_{k,m}$ bound a second embedded disc B' , with corners v_l, w_m, y_1, y_2 (Figure 6). We say the pair h_j, g_k are completed along B' . Note that, turning the picture upside-down, the pair $h_{l,j}, g_{m,k}$ is initially parallel along B' , and completed along B .

As an intuition-building observation, and justification of the term 'singular annulus', note that if initially parallel h_j, g_k are completed then the resolution of the points y_1, y_2 as in Figure 7 transforms the 'singular' $B \cup B'$ into an immersed annulus.

We have come to the key definition of this section:

Definition 3.6. Let $\{\gamma_i\}_{i=1}^n, n \geq 1$, be a collection of non-intersecting, properly embedded arcs in Σ , φ a right-veering monodromy in Γ_Σ , and $\mathcal{P}_i = \mathcal{P}_i(\varphi, \gamma_i)$ a right position for each i . We say the \mathcal{P}_i are consistent if for all $j \neq k$, $h \in H(\mathcal{P}_j), g \in H(\mathcal{P}_k)$ are completed whenever they are initially parallel. For the case $n = 2$, we say $(\gamma_1, \varphi(\gamma_1)), (\gamma_2, \varphi(\gamma_2))$ are a right pair if they admit consistent right positions $\mathcal{P}_1, \mathcal{P}_2$.

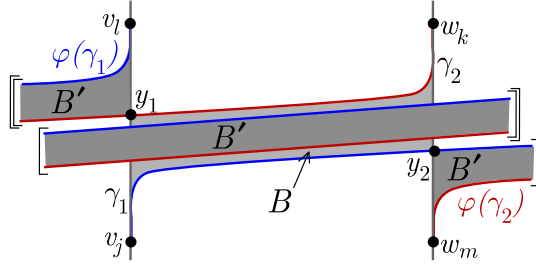


FIGURE 6. The horizontal segments h_j, g_k are completed by points v_l, w_m . Strands which terminate in like brackets are meant to be identified along arcs which are not drawn; a similar convention will be used throughout the paper.

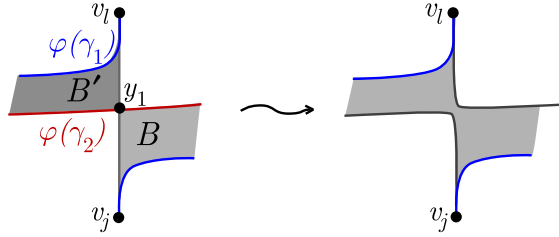


FIGURE 7. resolution of y_1

Example 3.7. The pair $(\gamma_1, \varphi(\gamma_1)), (\gamma_2, \varphi(\gamma_2))$ in Figure 8(a), with the right positions indicated, is a right pair, with two completed pairs of horizontal arcs, as indicated in (b). It is straightforward to verify that there are no other initially parallel segments.

The pair in Figure 9, however, is not a right pair: Suppose $\mathcal{P}_1, \mathcal{P}_2$ are consistent right positions. Then h_0, g_0 are initially parallel along B , so there must be $v_1 \in \mathcal{P}_1, w_1 \in \mathcal{P}_2$ satisfying the compatibility conditions. The only candidates are c'_1, c'_2 , and these do not give completed horizontal segments. Note that, by Theorem 3.1, this is sufficient to conclude that the mapping class has no positive factorization.

3.1. The right position associated to a factorization. Suppose we have a surface Σ , a mapping class $\varphi \in \Gamma_\Sigma$ given as a factorization ω of positive Dehn twists, and a set $\{\gamma_i\}_{i=1}^n$ of pairwise non-intersecting, properly embedded arcs in Σ . While each such arc admits at least one, and possibly many, right positions, the goal of this subsection is to give an algorithm which associates to ω a unique right position $\mathcal{P}(\omega, \gamma_i)$ for each i , such that the set $\{\mathcal{P}(\omega, \gamma_i)\}_{i=1}^n$ is consistent (Definition 3.6). Note that existence of such an algorithm proves Theorem 3.1.

We begin with the case of a single arc γ , and construct $\mathcal{P}(\omega, \gamma)$ by induction on the number of twists m in ω .

Base step: $m = 1$ Suppose $\varphi = \tau_\alpha$, for some $\alpha \in SCC(\Sigma)$. We begin by isotoping α so as to minimize $\#\alpha \cap \gamma$. Label $\alpha \cap \gamma = \{x_1, \dots, x_p\}$, with indices increasing along γ . We then define the right position $\mathcal{P}(\tau_\alpha, \gamma)$ associated to the factorization τ_α to be the points $\{c = v_0, v_1, \dots, v_{p-1}, c' = v_p\}$, where $\{c, c'\} = \partial(\gamma)$,

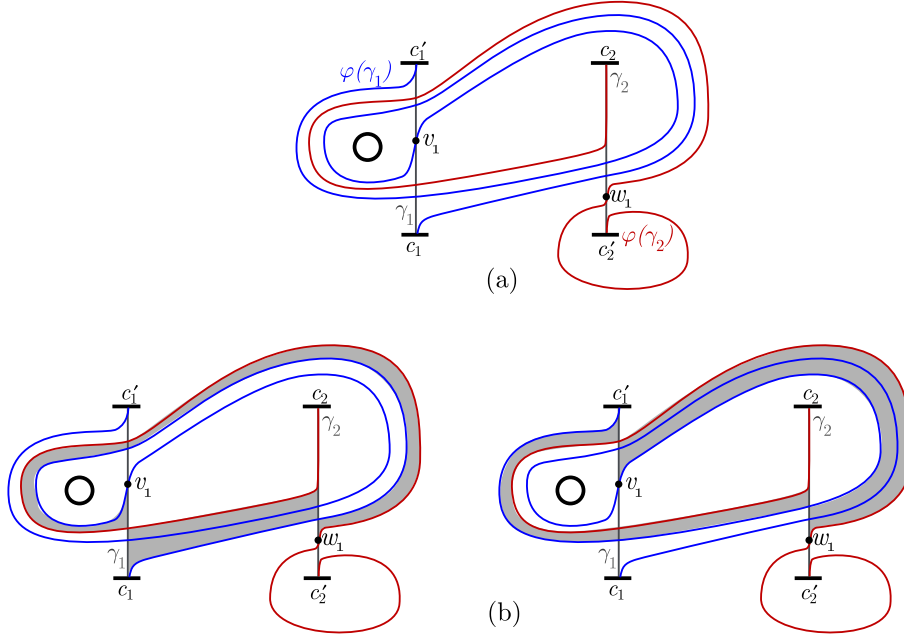


FIGURE 8. (a) : $(\gamma_1, \varphi(\gamma_1)), (\gamma_2, \varphi(\gamma_2))$ is a right pair. The pairs of completing discs are shaded in (b).

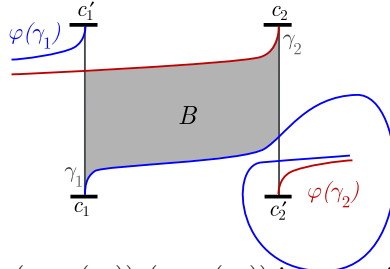


FIGURE 9. $(\gamma_1, \varphi(\gamma_1)), (\gamma_2, \varphi(\gamma_2))$ is *not* a right pair.

and, for $0 < i < p$, v_i lies in the connected component of $\gamma \setminus \text{support}(\tau_\alpha)$ between x_i and x_{i+1} (Figure 10).

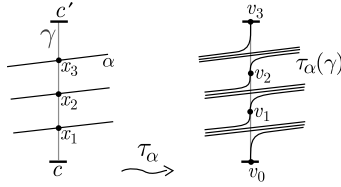


FIGURE 10. The base case: the right position $\mathcal{P}(\tau_\alpha, \gamma)$ associated to a single Dehn twist.

As an aside, note that, in this case, if $\bar{h}_{i,j}$ denotes the ‘closure’ of the horizontal segment $h_{i,j}$ obtained by adding the segment along γ from v_i to v_j to get a closed curve, then $\bar{h}_{i,i+1} \simeq \alpha$ for $0 \leq i < p$.

Now, this construction has as input only the isotopy class of α , so we have:

Lemma 3.8. *The right position $\mathcal{P}(\tau_\alpha, \gamma)$ defined in **base step** depends only on the isotopy class of α .*

3.1.1. *Description of the inductive step.* For the inductive step, we demonstrate an algorithm which has as input a surface Σ , mapping class $\varphi \in \Gamma_\Sigma$, properly embedded arc $\gamma \hookrightarrow \Sigma$, right position $\mathcal{P}(\varphi, \gamma)$, and $\alpha \in SCC(\Sigma)$. The output then will be a unique right position $\mathcal{P}^\alpha = \mathcal{P}^\alpha(\tau_\alpha \circ \varphi, \gamma)$. A key attribute of the algorithm will be that, while α is given as a particular representative of its isotopy class $[\alpha]$, the resulting right position \mathcal{P}^α will be independent of choice of representative.

To keep track of things in an isotopy-independent way, we consider *triangular regions* in Σ :

Definition 3.9. *Suppose γ, γ' are properly embedded arcs in a surface Σ such that $\partial(\gamma) = \partial(\gamma')$, isotoped to minimize intersection. Then for $\alpha \in SCC(\Sigma)$, a triangular region T (of the triple $(\gamma, \gamma', \alpha)$) is the image of an embedding $f : \Delta \hookrightarrow \Sigma$, where Δ is a 2-simplex with vertices t_1, t_2, t_3 and edges t_1t_2, t_2t_3, t_3t_1 , such that $f(t_1t_2) \subset \gamma$, $f(t_2t_3) \subset \gamma'$, and $f(t_3t_1) \subset \alpha$.*

Definition 3.10. *A triangular region T for the ordered triple $(\alpha, \gamma, \gamma')$ is*

- essential if α can be isotoped relative to $T \cap \alpha$ so as to intersect γ, γ' in a minimal number of points (Figure 14(a)).
- upward (downward) if bounded by α, γ, γ' in clockwise (counterclockwise) order (Figure 14(b)).

We begin with a brief description of the algorithm, with an illustrative example in Figure 11. Let α be a representative of $[\alpha]$ which minimizes $\alpha \cap \gamma$ and $\alpha \cap \varphi(\gamma)$, so in particular all triangular regions for the triple $(\alpha, \gamma, \varphi(\gamma))$ are essential. Furthermore, chose $support(\tau_\alpha)$ so as not to intersect any point of $\gamma \cap \varphi(\gamma)$ (Figure 11(a)). Consider then the image $\tau_\alpha(\varphi(\gamma))$, which differs from $\varphi(\gamma)$ only in $support(\tau_\alpha)$ (Figure 11(b)). Now, the only bigons bounded by the arcs $\tau_\alpha(\varphi(\gamma))$ and γ contain vertices which were in upward triangles in the original configuration. In particular, there is an isotopy of $\tau_\alpha(\varphi(\gamma))$ over (possibly some subset of) these bigons which minimizes $\gamma \cap \tau_\alpha(\varphi(\gamma))$ (the issue of exactly when a proper subset of the bigons suffices is taken up below, in Section 3.1.2). There is thus an inclusion map i of those points of \mathcal{P} which are *not* in upward triangles into the set of positive intersections of $\gamma \cap \tau_\alpha(\varphi(\gamma))$, whose image is therefore a right position (Figure 11(c)).

Note however that, as described, this resulting right position is *not* independent of the choice of α - indeed, if T_1 is any downward triangle, we may isotope the given α over T_1 (Figure 11(d)) to obtain $\alpha' \in [\alpha]$ such that $\alpha' \cap \gamma$ and $\alpha' \cap \varphi(\gamma)$ are also minimal. This new α' thus satisfies the conditions of the algorithm, yet the algorithm of the previous paragraph determines a distinct right position for $\gamma, \tau'_\alpha(\varphi(\gamma))$ (Figure 11(f)). Motivated by this observation, we refine the algorithm by adding *all* points of $\gamma \cap \tau_\alpha(\varphi(\gamma))$ which would be obtained by running the algorithm for any allowable isotopy of α (Figure 11(g)). As we shall see, this simply involves adding including a single point for each downward triangle in the original configuration.

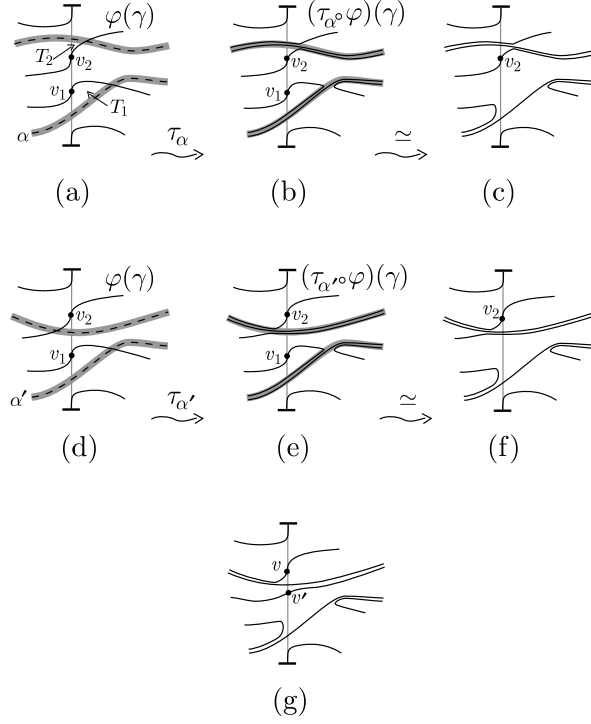


FIGURE 11. Top row: (a) The setup for the above discussion. T_1 is an upward, T_2 a downward triangular region. The support of the twist τ_α is shaded. (b) The result of τ_α . There is a single bigon, in which v_1 is a vertex. (c) The result of isotoping $\tau_\alpha(\varphi(\gamma))$ over this bigon so as to minimize intersection with γ . Bottom row: Same as the top, but with α' . Note that while the images $\tau_\alpha(\varphi(\gamma))$, $\tau_{\alpha'}(\varphi(\gamma))$ are of course isotopic, the right positions of (c) and (f) differ. Finally, (g) indicates the isotopy-independent right position (i.e. the points v, v' , along with $\partial\gamma$) which our algorithm is meant to pick out.

3.1.2. *Details of the inductive step.* This subsection gives the technical details necessary to make the algorithm work as advertised, and extracts and proves the various properties we will require the algorithm and its result to have.

We begin with some results concerning triangular regions. Let γ, γ' be properly embedded, non-isotopic arcs in Σ , with $\partial(\gamma) = \partial(\gamma')$, isotoped to minimize intersection. Our motivating example, of course, is the case $\gamma' = \varphi(\gamma)$, so we orient the arcs as in Figure 2. Let \mathcal{G} denote their union. A *vertex* of \mathcal{G} is thus an intersection point $\gamma \cap \gamma'$. Let $\alpha \in SCC(\Sigma)$ be isotoped so as not to intersect any vertex of \mathcal{G} . A *bigon* in this setup is an embedded disc B bounded by α, γ or α, γ' (so, in particular, a triangular region is not a bigon). Similarly, a *bigon chain* is a set $\{B_i\}_{i=1}^n$ of bigons bounded exclusively by one of the pairs $(\alpha, \gamma), (\alpha, \gamma')$, for which the union $\bigcup\{\alpha \cap \partial(B_i)\}_{i=1}^n$ is a connected segment of α (Figure 12(a)). Finally, we say points $p, p' \in \alpha \cap \mathcal{G}$ are *bigon-related* if they are vertices in a common bigon chain.

Suppose then that T is a triangular region in this setup, with vertex $v \in \gamma \cap \gamma'$. We define the *bigon collection associated to T* , denoted \mathcal{B}_T , as the set of points $\{p \in \alpha \cap \mathcal{G} \mid p \text{ is bigon-related to a vertex of } T\}$ (Figure 12(b)). Note that, if a vertex of T is not a vertex in any bigon, the vertex is still included in \mathcal{B}_T , so that, for example, the bigon collection associated to an essential triangle T is just the vertices of T .

Now, the point v divides each of γ, γ' into two segments, which we label $\gamma_+, \gamma_-, \gamma'_+, \gamma'_-$ in accordance with the orientation. For each bigon collection \mathcal{B} associated to a triangle with vertex v , we define $\sigma_v(\mathcal{B}) := (|\mathcal{B} \cap \gamma_+|, |\mathcal{B} \cap \gamma_-|, |\mathcal{B} \cap \gamma'_+|, |\mathcal{B} \cap \gamma'_-|) \in (\mathbb{Z}_2)^4$, where intersections numbers are taken mod 2 (Figure 12(b)).

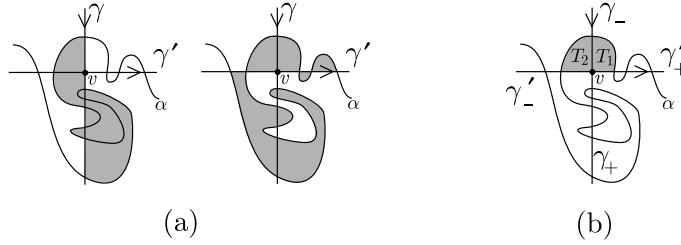


FIGURE 12. (a) The shaded regions are distinct maximal bigon chains. (b) As each chain from (a) has a vertex in each of the triangular regions T_1, T_2 , the bigon collection $\mathcal{B}_{T_1} = \mathcal{B}_{T_2}$ includes each vertex of each chain. $\sigma_v(\mathcal{B}_{T_1}) = (0, 1, 1, 0)$, so the collection is downward. Note that T_1 is an essential downward triangular region (Definition 3.10), while T_2 is non-essential and upward.

Finally, we label a bigon collection \mathcal{B} as *upward* (with respect to v) if $\sigma_v(\mathcal{B}) \in \{(1, 0, 1, 0), (0, 1, 0, 1)\}$, *downward* if $\sigma_v(\mathcal{B}) \in \{(1, 0, 0, 1), (0, 1, 1, 0)\}$, *non-essential* otherwise (Figure 12(b)).

Lemma 3.11. *Let $\alpha \in [\alpha]$ be such that $\alpha \cap \gamma, \alpha \cap \varphi(\gamma)$ are minimal, and $v \in \varphi(\gamma) \cap \gamma$. Then the number of essential triangles with vertex v in the triple $(\gamma, \varphi(\gamma), \alpha)$ depends only on the isotopy class $[\alpha]$.*

Proof. Let α be an arbitrary representative of $[\alpha]$, and v a vertex. We define an equivalence relation on the set of triangular regions with vertex v by $T_1 \sim T_2 \Leftrightarrow \mathcal{B}_{T_1} = \mathcal{B}_{T_2}$. In particular, there is a 1-1 correspondence between $\{\text{triangular regions with vertex } v\} / \sim$ and the set of bigon collections associated to triangular regions with vertex v .

Now, if α' is another representative of the isotopy class $[\alpha]$, we may break the isotopy into a sequence $\alpha = \alpha_1 \simeq \dots \simeq \alpha_n = \alpha'$, where each isotopy $\alpha_i \simeq \alpha_{i+1}$ is either a bigon birth, a bigon death, or does not affect either of $|\alpha \cap \gamma|, |\alpha \cup \varphi(\gamma)|$. Note that, if \mathcal{B} is upward or downward, an isotopy $\alpha_i \simeq \alpha_{i+1}$ which does not cross v does not affect $\sigma_v(\mathcal{B})$, while an isotopy $\alpha_i \simeq \alpha_{i+1}$ which crosses v changes $\sigma_v(\mathcal{B})$ by addition with $(1, 1, 1, 1)$. In either case, the classification is preserved; i.e. we can keep track of an essential upward (downward) bigon collection through each isotopy. Furthermore, any two distinct bigon collections will have distinct images under each such isotopy (a bigon birth/death cannot cause two maximal bigon chains to merge). We therefore have an integer $a(v)$, defined as the number of

essential bigon collections \mathcal{B} associated to triangular regions with vertex v , which depends only on $[\alpha]$

Finally, if we take α' to be a representative of $[\alpha]$ which intersects γ and $\varphi(\gamma)$ minimally, then $\{\text{triangular regions with vertex } v\} / \sim$ is by definition just the set of essential triangular regions with vertex v , and has size $a(v)$. \square

Lemma 3.12. *Let α be a fixed representative of the isotopy class $[\alpha]$ which has minimal intersection with $\gamma \cap \varphi(\gamma)$, $v \in \gamma \cap \varphi(\gamma)$ a vertex of an upward triangle T . Then v is not a vertex of any downward triangular region T' for α .*

Proof. Consider the neighborhood of v as labeled in Figure 13. As T is upward, it must be T_1 or T_3 , while T' must be T_2 or T_4 . Without loss of generality then suppose $T = T_1$ is a triangular region. But then neither of T_2, T_4 can be triangular regions without creating a bigon, violating minimality. \square

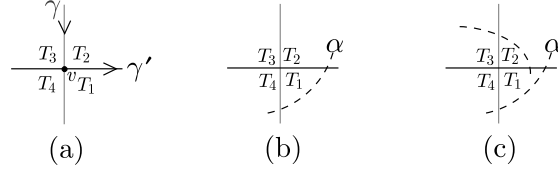


FIGURE 13. (a) A neighborhood of v . (b) The upward triangle T_1 . (c) As α has no self-intersection, T_2 cannot be a triangular region without creating a bigon.

It follows from Lemmas 3.11 and 3.12 that we may unambiguously refer to a vertex of an essential triangular region as downward, upward, or neither, in accordance with any essential triangular region of which it is a vertex. In particular, if α has minimal intersection with $\gamma, \varphi(\gamma)$, then all triangular regions are essential. Henceforth we will drop the adjective ‘essential’. Figure 14(b) and (c) give examples of the various types of vertices.

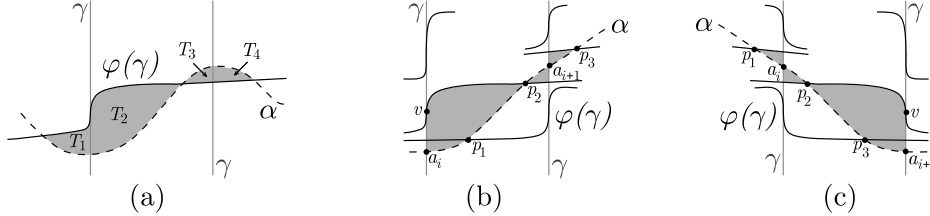
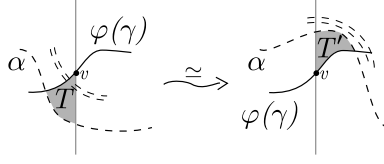


FIGURE 14. (a) T_1, T_4 are essential triangular regions for $(\alpha, \gamma, \gamma')$, T_2, T_3 are not. (b) Upward triangular regions and vertices. (c) Downward triangular regions and vertices.

Definition 3.13. *Suppose T is a triangular region with vertex $v \in \gamma \cap \varphi(\gamma)$. Isotope α over T to obtain another triangular region T' of the same type (upward/downward) as T with vertex v , as in Figure 15. Note that if T contains sub-regions with vertex v then the process involves isotoping the innermost region first, and proceeding to T itself. We call such an isotopy a shift over v .*


 FIGURE 15. A shift over a vertex v .

We require one final definition before we bring the pieces together:

Definition 3.14. *Suppose we have a properly embedded arc $\gamma \hookrightarrow \Sigma$, $\varphi \in \Gamma_\Sigma$, with $\varphi(\gamma), \gamma$ isotoped to minimize the number of connected components of $\gamma \cap \varphi(\gamma)$, $\alpha \in SCC(\Sigma)$, and $v \in \gamma \cap \varphi(\gamma)$ a positively oriented intersection point (again, these are not required to be transverse). Suppose further that for some representative of the isotopy class of α , the image $\tau_\alpha(\varphi(\gamma))$ can be isotoped to intersect γ in a minimal number of connected components while fixing a neighborhood of v . Then v is called fixable under τ_α (Figure 16). Similarly, for a factorization $\omega = \tau_{\alpha_n} \cdots \tau_{\alpha_1}$ of φ , we say $v \in \varphi(\gamma) \cap \gamma$ is fixable under ω if v is fixable under each successive τ_{α_i} .*

Observation 3.15. *Using this terminology, we have the following characterization of the right position $\mathcal{P}(\omega, \gamma)$ which the reader may or may not find helpful: The right position $\mathcal{P}(\omega, \gamma)$ is a minimal subset of the positive intersections in $\gamma \cap \varphi(\gamma)$ such that each point of $\mathcal{P}(\omega, \gamma)$ is fixable under ω , and is in fact the unique such position up to a choice involved in the coarsening process (described in detail in the proof of Lemma 3.18).*

As a simple example, Figure 17 illustrates distinct right positions of a pair $(\gamma, \varphi(\gamma))$ associated to distinct factorizations of φ .

We are now ready to precisely describe the inductive step. Let $\mathcal{P} = \mathcal{P}(\varphi, \gamma)$ be a right position, and let $\alpha \in SCC(\Sigma)$. We construct the right position $\mathcal{P}^\alpha = \mathcal{P}^\alpha(\tau_\alpha \circ \varphi, \gamma)$ in two steps. Firstly, we coarsen \mathcal{P} by removing all points which are not fixable by τ_α . This new right position, being fixable under τ_α , defines a right position for $\gamma, \tau_\alpha(\varphi(\gamma))$. Secondly we refine this new position by adding points so as to have each new fixable component of $\gamma \cap \tau_\alpha(\varphi(\gamma))$ accounted for.

Coarsening

The coarsening process takes the given right position \mathcal{P} and a curve $\alpha \in SCC(\Sigma)$, and returns a right position $\mathcal{P}' = \mathcal{P}'(\varphi, \gamma) \subset \mathcal{P}$. The intuitive idea is that we will remove the minimal subset of \mathcal{P} such that the remaining points can be simultaneously fixed by τ_α , thus allowing an identification with points in $\gamma \cap \tau_\alpha(\varphi(\gamma))$. Of course we must do so in a way which depends only on the isotopy class of α .

We begin by choosing a specific representative α of the isotopy class $[\alpha]$ which has minimal intersection with γ and $\varphi(\gamma)$. Choose $support(\tau_\alpha)$ to be disjoint from \mathcal{P} . Now, the only bigons bounded by the arcs $\tau_\alpha(\varphi(\gamma)), \gamma$ correspond to upward triangular regions of the original triple $(\gamma, \varphi(\gamma), \alpha)$. Thus, any isotopy which minimizes $|\tau_\alpha(\varphi(\gamma)) \cap \gamma|$ must isotope $\tau_\alpha(\varphi(\gamma))$ over some subset of the upward triangular regions. The coarsening must therefore consist of a removal of a subset of the upward points of \mathcal{P} . We want to determine which of these points are fixable under α .



FIGURE 16. (a) A downward point is fixable. (b) An upward point is *not* fixable, unless (c) there is another upward triangle sharing the other two vertices. Note that, in this case, while either of the points v, v' is individually fixable, the pair is not simultaneously fixable. Finally, (d) illustrates the reason for demanding that a *neighborhood* of the point be fixed - though the intersection-minimizing isotopy may be done without removing the intersection point v , there is no fixable neighborhood, and so v is not fixable.

Lemma 3.16. *Suppose that $v \in \mathcal{P}$ is a vertex of an upward triangular region T . Then if v is fixable under τ_α , then there is another upward triangular region T' such that T, T' share the vertices of T other than v (Figure 16(c)).*

Proof. Let a be the vertex of T at $\alpha \cap \gamma$, p the remaining vertex (Figure 18(a)). As v is upward, there is a bigon in the image, corresponding to T , bounded by $(\tau_\alpha \circ \varphi)(\gamma)$ and γ , with vertices v and a (Figure 18(b)). Therefore, if v is to be

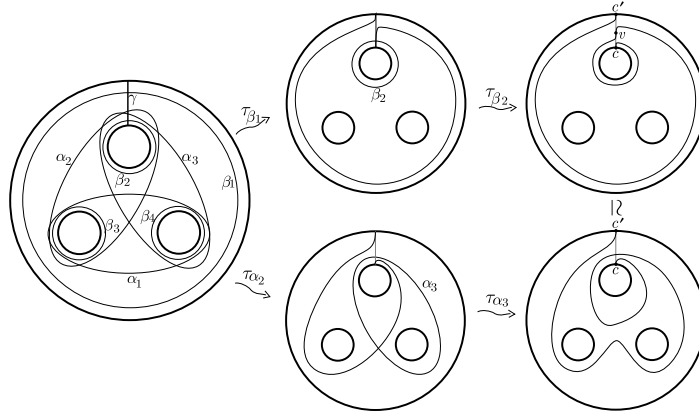


FIGURE 17. On the left are the curves of the well-known lantern relation on $\Sigma_{0,4}$ - setting $\omega_1 = \tau_{\beta_4}\tau_{\beta_3}\tau_{\beta_2}\tau_{\beta_1}$, $\omega_2 = \tau_{\alpha_3}\tau_{\alpha_2}\tau_{\alpha_1}$, the lantern relation tells us that ω_1, ω_2 are factorizations of a common $\varphi \in \Gamma_\Sigma$. Clearly, for the arc γ indicated, the intersection point $v \in \varphi(\gamma) \cap \gamma$ in the upper right figure is fixable under ω_1 . However, as is clear from the lower sequence of figures, v is *not* fixable under the factorization ω_2 . Thus the right position $\mathcal{P}(\omega_1, \gamma)$ contains the point v as well as the endpoints of γ , while $\mathcal{P}(\omega_2, \gamma)$ contains only the endpoints of γ .

fixed through an isotopy of $\tau_\alpha(\varphi(\gamma))$ which minimizes $\#\tau_\alpha(\varphi(\gamma)) \cap \gamma$, then a must be a vertex of a second bigon also bounded by $\tau_\alpha(\varphi(\gamma))$ and γ , with vertices a and v' for some $v' \in \tau_\alpha(\varphi(\gamma)) \cap \gamma$ (Figure 18(c)). By minimality of intersections in the original configuration, this new bigon then corresponds to a second upward triangle T' with vertices a, v', p' in the original configuration (Figure 18(d)). As v is fixable, the bigons must cancel, and we have $p = p'$, as desired (Figure 16(c) indicates the configuration). Note that, while each of v, v' is fixable, the pair is not *simultaneously* fixable. \square

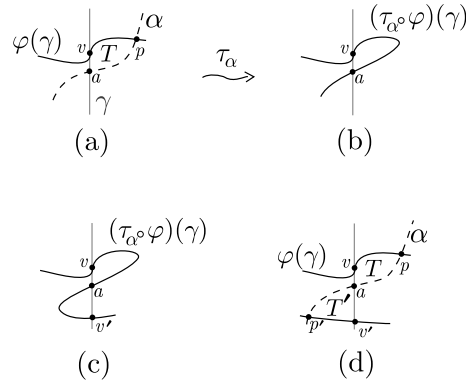


FIGURE 18. Figures for Lemma 3.16.

Also,

Lemma 3.17. *If triangular regions T, T' share exactly two vertices, then these vertices are the pair along α .*

Proof. Let the triples (v_1, p_1, a_1) , (v_2, p_2, a_2) be the vertices of upward triangles T_1, T_2 , where $v_i \in \gamma \cap \varphi(\gamma)$, $p_i \in \alpha \cap \varphi(\gamma)$, and $a_i \in \alpha \cap \gamma$, and suppose T_1, T_2 have exactly two vertices in common. Essential triangular regions can have no edges in common, so they can have two vertices in common only if the vertices lie along a closed curve given by the union of the two edges defined by the pair of vertices. In particular, as α is the only closed curve in the construction, the points in common must be $p_1 = p_2$ and $a_1 = a_2$. \square

Motivated by Lemmas 3.16 and 3.17, we introduce an equivalence relation \sim on the set of upward triangular regions, such that $T \sim T'$ if and only if they share exactly two vertices. To finish the coarsening process, we have:

Lemma 3.18. *Let \mathcal{P}' be a right position given by removing a single point of \mathcal{P} from each equivalence class in which each triangular region has a vertex in \mathcal{P} . Then \mathcal{P}' satisfies the following properties:*

- (1) *Each point of \mathcal{P}' is fixable under τ_α*
- (2) *\mathcal{P}' is a maximal subset of \mathcal{P} for which property (1) holds.*
- (3) *\mathcal{P}' depends only on the isotopy class of α .*

Proof. Let Ω be an equivalence class of upward triangles. We distinguish two subcases, depending on whether each element of Ω has a vertex in \mathcal{P} or not. To emphasize the distinction, we call a point $p \in \gamma \cap \varphi(\gamma)$ a *vertical point* if p is in \mathcal{P} , non-vertical otherwise.

- (1) (Each element of Ω has a vertex in \mathcal{P}) Let $T \in \Omega$. Using Lemma 3.17, the equivalence class of T is formed of triangles sharing the points along α (a typical equivalence class of three triangles is shown in the left side of Figure 19(a)). Suppose then that Ω contains m triangular regions. As noted in the proof of Lemma 3.16, at most $m - 1$ vertical points from the vertices of elements of Ω are simultaneously fixable under τ_α , and conversely, *any* set of $m - 1$ vertical points from these is fixable. In particular, if each triangle in the class has a vertex in \mathcal{P} , the removal of a single vertical point is a necessary and sufficient refinement of the vertical points involved in the equivalence class so as to satisfy properties (1) and (2). Clearly the resulting set \mathcal{P}' obtained by repeating this refinement on each equivalence class is independent (as an unordered set) of the actual choice of which vertical point to remove, and so property (3) is satisfied.
- (2) (Ω contains some element which does not have a vertex in \mathcal{P}) If there is a triangle in the class which does not have a vertex in \mathcal{P} , then all of the above goes through for the neighborhood of the non-vertical point p of $\varphi(\gamma) \cap \gamma$; i.e., the twist τ_α , along with any isotopy of the image $\tau_\alpha(\gamma)$ necessary to minimize intersections can be done relative to a neighborhood of each vertical point, so that there is no coarsening necessary. There is however a choice involved if there are two non-consecutive (i.e., separated by a vertical point) non-vertical points in the class (Figure 19 is a typical example). As we shall see, this choice has no effect on the consistency of resulting positions, but for convenience we dispose of the ambiguity by

removing the non-vertical point *furthest* along $\varphi(\gamma)$ from the distinguished endpoint $c \in \partial\gamma$. Again, property (3) follows immediately. \square

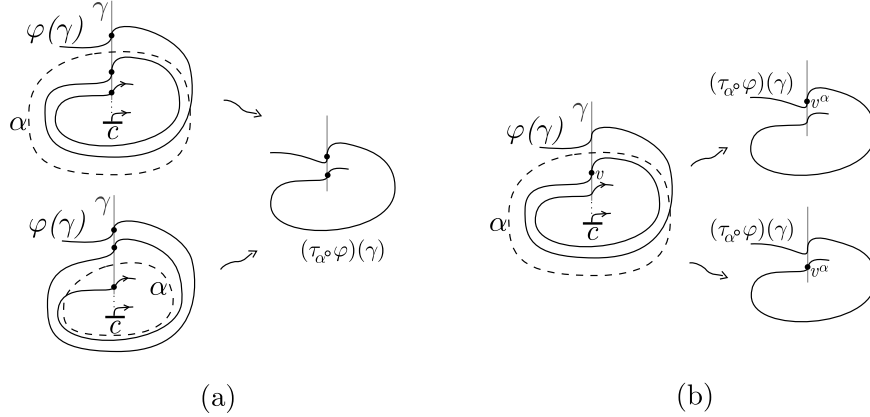


FIGURE 19. (a) For the case that each element of an equivalence class has a vertical vertex, α can be isotoped so as to fix all but any single vertical point - the result is independent of the choice of which subset to fix. (b) An upward equivalence class of triangles whose set of vertices contain non-consecutive (along γ), non-vertical points of $\gamma \cap \varphi(\gamma)$ (here separated by the vertical point v). There is therefore a choice of vertical point in the image. Our convention will be to choose the lower figure.

Lemma 3.19. *The right position $\mathcal{P}' \subset \mathcal{P}$ of $(\gamma, \varphi(\gamma))$, resulting from the coarsening process, (a) depends only on the isotopy class of α , and (b) is simultaneously fixable under τ_α .*

Proof. Claim (a) is Property (3) of Lemma 3.18.

For (b), we again consider the effect of the Dehn twist τ_α restricted to a supporting neighborhood of the twist chosen so as not to intersect any point of $\gamma \cap \varphi(\gamma)$. Observe then that in the image, the only bigons bounded by the curves $(\tau_\alpha \circ \varphi)(\gamma), \gamma$ correspond to essential upward triangles in the original configuration. Each singleton equivalence class contributes a single, isolated bigon, while classes with multiple elements contribute canceling pairs of bigons. In particular, $|\gamma \cap (\tau_\alpha \circ \varphi)(\gamma)|$ may be minimized by an isotopy of $\tau_\alpha(\varphi(\gamma))$ over one bigon from each class. This isotopy fixes a neighborhood of each of the points \mathcal{P}' . \square

Refinement

For the final step, we wish to identify the right position \mathcal{P}' given by the coarsening process as a right position for $(\gamma, \tau_\alpha(\varphi(\gamma)))$, and then to refine by adding points to obtain the desired right position \mathcal{P}^α for $(\gamma, \tau_\alpha(\varphi(\gamma)))$.

So, let α be a given representative of the isotopy class $[\alpha]$ such that the sets $\alpha \cap \gamma, \alpha \cap \varphi(\gamma)$ are minimal. By Lemma 3.19, the set \mathcal{P}' is simultaneously fixable

under τ_α , so we have a canonical identification of \mathcal{P}' as a subset $i_\alpha(\mathcal{P}')$ of the positive intersections of $\tau_\alpha(\varphi(\gamma)) \cap \gamma$, and thus as a right position for $(\gamma, \tau_\alpha(\varphi(\gamma)))$.

As we are after an isotopy-independent result, we shall require that \mathcal{P}^α include each point which is fixed by *any* representative of $[\alpha]$ which satisfies the intersection-minimality conditions. So, let $v \in \mathcal{P}'$ be a downward point. Then for each vertical downward triangular region T with vertex v , let a be the vertex $\alpha \cap \gamma$. We label the positive intersection of $\gamma, (\tau_\alpha \circ \varphi)(\gamma)$ corresponding to a by $d_{a,v} \in (\tau_\alpha \circ \varphi)(\gamma) \cap \gamma$ (Figure 20), and call the set of all such points V_v . We refer to $i_\alpha(v) \cup V_v \subset \mathcal{P}^\alpha$ as *the refinement set corresponding to v* . Note that, for distinct v, v' , the sets $V_v, V_{v'}$ are not necessarily disjoint, but as we only require that each such point be accounted for, this does not affect the construction. We now define the right position \mathcal{P}^α of $(\gamma, \tau_\alpha(\varphi(\gamma)))$ as the union of all the refinement sets of each point, $\mathcal{P}^\alpha := i_\alpha(\mathcal{P}') \cup \{V_v | v \in \mathcal{P}'\}$.

Finally,

Lemma 3.20. *The right position \mathcal{P}^α of $(\gamma, \tau_\alpha(\varphi(\gamma)))$ given by the refinement process, as an unordered set, depends only on the isotopy class of α .*

Proof. Suppose α, α' are fixed representatives of a given isotopy class of simple closed curves, each intersecting $\gamma \cup \varphi(\gamma)$ minimally. Then, by Lemma 3.11, for $v \in \mathcal{P}'$, the number of downward triangular regions with vertex v is the same for α and α' . So, if v is a vertex of n downward triangular regions, then the refinement set corresponding to v for either curve will consist of the same $n + 1$ element subset of $\tau_\alpha(\varphi(\gamma)) \cap \gamma$, so that their union \mathcal{P}^α depends only on $[\alpha]$, as desired. Notice that $i_\alpha(v) \neq i_{\alpha'}(v)$ exactly when the number of triangles above/below v differs for α and α' . In particular, there is a sequence of shifts of α over v such that $i_\alpha(v) = i_{\alpha'}(v)$ (Figure 21). \square

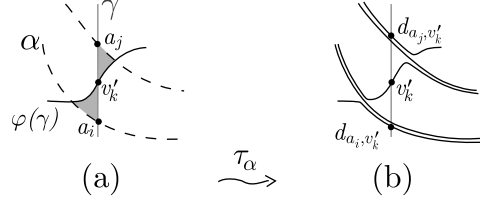


FIGURE 20. Construction of the set $V_{v'_k}$ for downward $v'_k \in \mathcal{P}'$. Figure (a) is the setup in \mathcal{P}' , (b) shows the result of the refinement for \mathcal{P}^α by vertical points $V_{v'_k} = \{d_{a_i, v'_k}, d_{a_j, v'_k}\}$ on $\tau_\alpha(\varphi(\gamma))$.

Definition 3.21. *Let $\varphi \in \Gamma_\Sigma$ be given s a positive factorization ω . The unique right position given to the pair $\gamma, \omega(\gamma)$ by the algorithm detailed in this section is the right position associated to ω , denoted $\mathcal{P}_\omega(\gamma)$.*

To finish things off, we need to extend the associated right position to each pair $\gamma_i, \varphi(\gamma_i)$ for an arbitrary set $\{\gamma_i\}$ of nonintersecting properly embedded arcs. We have:

Lemma 3.22. *Let $\{\gamma_i\}$ be a set of pairwise non-intersecting properly embedded arcs in Σ . The algorithm as given above extends to an algorithm which assigns a unique right position $\mathcal{P}_\omega(\gamma_i)$ to each pair $\gamma_i, \varphi(\gamma_i)$.*

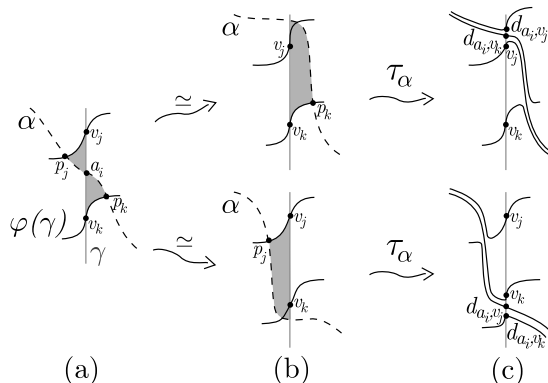


FIGURE 21. \mathcal{P}^α is independent of isotopy of α in the refinement process. (a) is the initial setup, with $p_j, p_k \in \alpha \cap \varphi(\gamma)$, (b) indicates distinct isotopies, and (c) is the resulting \mathcal{P}^α for each choice. While the labeling is different, the configurations are isotopic.

Proof. This follows directly from independence of the algorithm from the choice of representative of the isotopy class of α , and the fact that we may always find some representative of α which intersects each of $\{\gamma_i\}, \{\varphi(\gamma_i)\}$ minimally. \square

3.2. Consistency of the associated right positions. The goal of this subsection is to show that any two right positions $\mathcal{P}_\omega(\gamma_1), \mathcal{P}_\omega(\gamma_2)$ associated to a positive factorization ω are consistent (Definition 3.6). Theorem 3.1 will follow from this result, coupled with Lemma 3.22.

Our method to show consistency will be to use the right positions to ‘localize’ the situation. Recall from the previous section (in particular the proof of Lemma 3.20) that, if $\mathcal{P} \rightsquigarrow \mathcal{P}^\alpha$ denotes the algorithm, then, using the notation of that section, there is a representative α of $[\alpha]$ such that a given point of \mathcal{P}^α is in the image of the inclusion map $i_\alpha : \mathcal{P}' \rightarrow \mathcal{P}^\alpha$. In particular, this identification will hold for any isotopy of α which does not cross the preimage of our point. Thus, having fixed α up to this constraint, we may consider the preimage of such a point as having properties analogous to the endpoints of γ ; i.e. it is fixed by τ_α , and α cannot be isotoped so as to cross it.

Suppose then that we have a *pair* of nonintersecting properly embedded arcs on a surface with a given monodromy, with a pair of right positions $\mathcal{P}_1, \mathcal{P}_2$. Then, for a Dehn twist τ_α , the inductive step of the algorithm gives a pair $\mathcal{P}_1^\alpha, \mathcal{P}_2^\alpha$. Consider a *pair* of points, one from each of \mathcal{P}_i^α . We wish to show that the consistency conditions hold for each such pair; i.e. that the horizontal segments originating at the pair of points are completed if initially parallel. Now, if there is an isotopy of α such that each point is in the image of the associated inclusion map i_α (we call such a pair ‘simultaneous images’), then the horizontal segments have well-defined preimages in $\mathcal{P}_1, \mathcal{P}_2$, so we only have to understand the ‘local picture’ of the images under τ_α of each such pair.

As it turns out, pairs which are simultaneous images completely determine consistency:

Lemma 3.23. *Let \mathcal{P}_i be a right position for $(\gamma, \varphi(\gamma_i))$ $i = 1, 2$, $\alpha \in SCC(\Sigma)$, and \mathcal{P}_i^α the right position for $(\gamma, \tau_\alpha(\varphi(\gamma_i)))$ given by the algorithm. Suppose that, for each simultaneous image pair $v^\alpha \in \mathcal{P}_1^\alpha, w^\alpha \in \mathcal{P}_2^\alpha$, the horizontal segments h^α, g^α satisfy the consistency conditions (i.e. are completed whenever initially parallel). Then the positions $\mathcal{P}_1^\alpha, \mathcal{P}_2^\alpha$ are consistent.*

Proof. We need to show that, if each initially parallel pair of horizontal segments whose initial points are a simultaneous image is completed, then the same is true of each initially parallel pair of horizontal segments whose initial points are not a simultaneous image. So, let h^α, g^α be horizontal segments whose initial points $v^\alpha \in \mathcal{P}_1^\alpha, w^\alpha \in \mathcal{P}_2^\alpha$ cannot be a simultaneous image.

Now, by Lemma 3.20, for any α and any pair $v^\alpha \in \mathcal{P}_1^\alpha, w^\alpha \in \mathcal{P}_2^\alpha$, there is $v_j \in \mathcal{P}_1, w_k \in \mathcal{P}_2$ such that, after a shift of α over v_j or w_k , we can arrange $v^\alpha = i(v_j)$ or $w^\alpha = i(w_k)$. A pair is thus not a simultaneous image if and only if these shifts cannot be done simultaneously in a way which preserves the minimality of intersections which the algorithm requires of α .

Suppose then that we have fixed α so that $v^\alpha = i(v_j)$. So, the identification $v^\alpha = i(v_j)$ will hold for any isotopy of α which preserves minimality of intersections and which does not cross the point v_j . These conditions are then an obstruction to shifting α over w_k only if v_j is in the interior of the triangular region T over which this shift is to occur (Figure 22(a)).

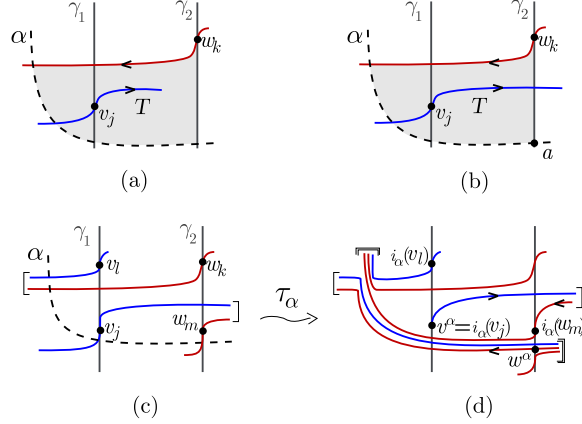


FIGURE 22. Figures for Lemma 3.23. There is no isotopy of α such that the points v^α, w^α indicated in (d) are each in the image of i_α .

Suppose, then, that v_j is in the interior of T . Consulting Figure 22(a), there is a unique way to complete the figure without introducing any bigons (Figure 22(b)). So, this determines our local picture, and w^α corresponds to the vertex a of T (Figure 22(b)) as described in the refinement process. In particular, the segment h_j lies within T , and so h_j, g_k are initially parallel. As $\mathcal{P}_1, \mathcal{P}_2$ are consistent, the segments are then completed to points $v_l \in \mathcal{P}_1, w_m \in \mathcal{P}_2$ (Figure 22(c)).

For reference, we have also drawn the (local) image under τ_α in Figure 22(d).

The information which Figure 22(d) is meant to convey is that, using the notation set in the previous paragraph, if v^α, w^α are not a simultaneous image, then the

part of the horizontal segment h^α from its initial point $v^\alpha = i_\alpha(v_j)$ up to the point $i_\alpha(v_l)$ is *not* initially parallel to the segment of g^α extending from initial point w^α to $i_\alpha(w_m)$. So, if h^α, g^α are initially parallel along some disc B , the points $i_\alpha(v_l), i_\alpha(w_m)$ must each be in ∂B . Now, these points are all in the image of i_α , thus by assumption the associated horizontal segments are completed whenever initially parallel. However, in this situation, it follows with little effort from Definition 3.5 that the segments h^α, g^α are themselves completed. To ease notation, we separate the argument as Lemma 3.24. \square

Lemma 3.24. *Suppose γ_1, γ_2 are non-intersecting, properly embedded arcs in a surface Σ , $\varphi \in \Gamma_\Sigma$, and \mathcal{P}_i a right position for each pair $(\gamma, \varphi(\gamma_i))$ $i = 1, 2$. Given $v_1, v_2 \in \mathcal{P}_1$, and $w_1, w_2 \in \mathcal{P}_2$, suppose the horizontal segments h_1, g_1 are initially parallel along a disc B , and that ∂B contains the segments $h_{1,2}, g_{1,2}$. (Figure 23(a)). Then if the pairs h_1, g_2 and h_2, g_1 are completed, so is h_1, g_1 .*

Proof. This follows from Definition 3.5 if one is able to keep track of everything. The steps are indicated in Figure 23.

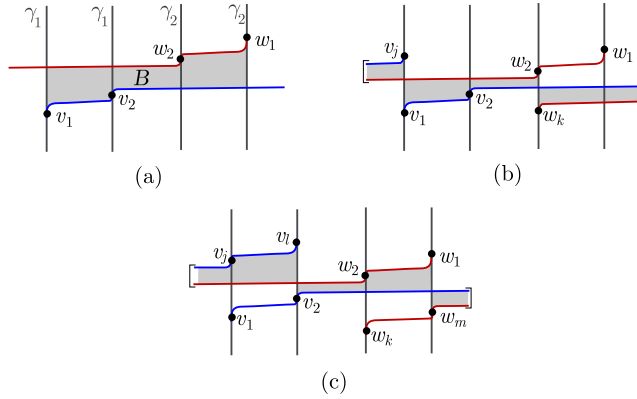


FIGURE 23. (a) is the setup, a neighborhood of the disc along which h_1, g_1 are initially parallel. Now, as the pair h_1, g_2 is assumed completed, there are endpoints v_j, w_k as in (b). Similarly, using the pair h_2, g_1 , we have endpoints v_l, w_m as in (c). But then h_1, g_1 are completed by v_j, w_m .

\square

We therefore only need concern ourselves with pairs of horizontal segments in $H(\mathcal{P}_1^\alpha), H(\mathcal{P}_2^\alpha)$ whose initial points have simultaneous preimages. In particular, it suffices to check that for any pair $h_j \in H(\mathcal{P}_1), g_k \in H(\mathcal{P}_2)$ with fixable initial points v_j, w_k , the images $\tau_\alpha(h_j), \tau_\alpha(g_k)$ are completed if initially parallel.

In keeping with analogy of fixable points as boundary points, we generalize the notion of ‘to the right’ (as presented in [HKM]) to arcs with common endpoint on the interior of a properly embedded arc γ :

Definition 3.25. *Let γ be a properly embedded arc in Σ , $\nu, \nu' : [0, 1] \hookrightarrow \Sigma$ embedded arcs in Σ with common endpoint $\nu(0) = \nu'(0) = x \in \gamma$, isotoped to minimize intersection, each to the same side of γ (i.e. if we fix a lift $\tilde{\gamma}$ in the universal cover*

$\tilde{\Sigma}$ of Σ , then $\tilde{\nu}, \tilde{\nu}'$ lie in the same connected component of $\tilde{\Sigma} \setminus \tilde{\gamma}$. We say ν' is to the right of ν' (at x), denoted $\nu' \geq \nu$, if either the pair is isotopic, or if the tangent vectors $(\nu'(0), \nu(0))$ define the orientation of Σ at x .

We first of all dispense with the case that the preimages h_j, g_k are not initially parallel.

Lemma 3.26. *Let γ_1, γ_2 be non-intersecting, properly embedded arcs in Σ , $\varphi \in \Gamma_\Sigma$, and \mathcal{P}_i a right position for $\gamma_i, \varphi(\gamma_i)$, $i = 1, 2$. Suppose $v_j \in \mathcal{P}_1, w_k \in \mathcal{P}_2$ are fixable under τ_α , and $h_j \in H(\mathcal{P}_1), g_k \in H(\mathcal{P}_2)$ are not initially parallel. Then if the images $\tau_\alpha(h_j), \tau_\alpha(g_k)$ are initially parallel, they are completed.*

Proof. Let Δ be the (unique up to isotopy) embedded arc with endpoints $i_\alpha(v_j), i_\alpha(w_k)$ which lies within the embedded disc along which $\tau_\alpha(h_j), \tau_\alpha(g_k)$ are initially parallel. So Δ also defines an arc (also denoted Δ) in the preimage configuration with endpoints v_j, w_k , which can be compared (in the sense of Definition 3.25) to h_j at v_j , and to g_k at w_k .

Suppose then that $h_j \geq \Delta$ (at v_j). Now, as $\tau_\alpha(h_j) \geq h_j$, and the image is to be initially parallel along Δ , then an initial segment of h_j up to γ_2 must be isotopic to Δ ; i.e there is an embedded triangular region T_1 with vertex v_j for which Δ is a side, and the other sides are subarcs of γ_2 , and h_j . Now, $g_k \cap h_j = \emptyset$, so $g_k \geq \Delta$ (at w_k), and thus by the same argument there is a triangle T_2 with vertex w_k , sides Δ, γ_1, g_k such that $T_1 \cup T_2$ is a disc along which h_j, g_k are initially parallel, contradicting our hypothesis.

So, Δ is to the right of each horizontal segment at its endpoints. For the image $\tau_\alpha(h_j)$ to lie along Δ , we may assume that α runs from γ_1 to γ_2 within a neighborhood of Δ , intersecting Δ exactly once. The same holds for $\tau_\alpha(g_k)$. There are then $v_l^\alpha \in \mathcal{P}_1^\alpha, w_m^\alpha \in \mathcal{P}_2^\alpha$ corresponding to the vertices $\alpha \cap \gamma_i$ of the associated triangles (Figure 24). The segments $\tau_\alpha(h_j), \tau_\alpha(g_k)$ are compatible, initially parallel along Δ with completing disc along the remainder of α and endpoints v_l^α, w_m^α . \square

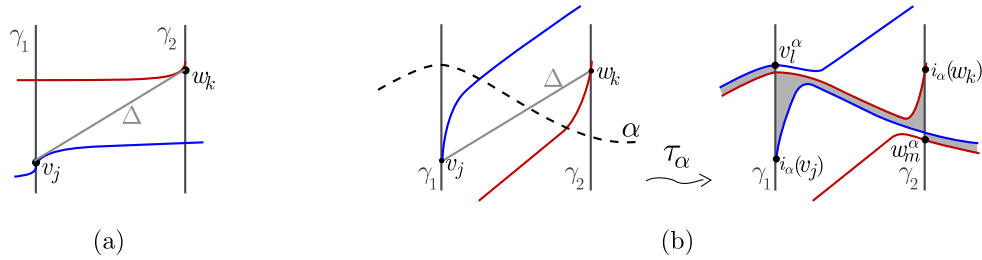


FIGURE 24. (a) If $h_j \geq \Delta$ (at v_j), then the same is true of g_k (at w_k), so the pair is initially parallel along Δ . (b) $\tau_\alpha(h_j), \tau_\alpha(g_k)$ are compatible, with endpoints v_l^α, w_m^α , given by the refinement procedure, corresponding to the points $\alpha \cap \gamma_i$

We are left with the case of initially parallel, and thus completed, horizontal segments h_j, g_k (again, Figure 6 indicates the situation). We need to show that the images of any such pair are completed whenever they are initially parallel.

Lemma 3.27. *Let γ_1, γ_2 be non-intersecting, properly embedded arcs in Σ , $\varphi \in \Gamma_\Sigma$, and \mathcal{P}_i a right position for $(\gamma_i, \varphi(\gamma_i))$, $i = 1, 2$. Suppose vertical points $v_j \in \mathcal{P}_1, w_k \in \mathcal{P}_2$ are fixable under τ_α , and the horizontal segments $h_j \in H(\mathcal{P}_1), g_k \in H(\mathcal{P}_2)$ are initially parallel and completed, with endpoints v_l, w_m . Then if the images $\tau_\alpha(h_j), \tau_\alpha(g_k)$ are initially parallel, they are completed.*

Proof. Following the above discussion, it suffices to consider the local picture of horizontal segments h_j, g_k , which remains valid for any (intersection minimizing) isotopy of a given α which does not cross v_j or w_k . We will refer to the notation of Figure 6. In particular, h_j, g_k are initially parallel along a disc B , and completed along a disc B' by endpoints v_l, w_m as in the Figure.

Our method of proof will depend on a classification of points of intersection $\alpha \cap h_j$ or $\alpha \cap g_k$. We will use the terminology of Definition 3.10, and consider triangular regions of the triples (γ_1, h_j, α) and (γ_2, g_k, α) . We call a point p in $\alpha \cap h_j$ or $\alpha \cap g_k$ *isolated* if it is a vertex in at most one triangular region. We will also continue to use the terminology of upward/downward, so that an intersection point is upward (downward) if it is a vertex in an upward (downward) triangle, as in Definition 3.10. Note that, as α is assumed to intersect each arc minimally, each triangle is essential.

Suppose firstly that there is a point $p \in \alpha \cap h_j$ which is isolated and a vertex in a downward triangular region in which one of the initial points v_j, w_k , say v_j , is also a vertex (so $p \in \alpha \cap h_j$). We call such p an *isolated initial downward point* (the point p in Figure 25(a) is a typical example). Note that, if such a point exists, then the intersection point closest to v_j (along h_j) must be of this type, so we may assume p is the closest point.

Now, as p is isolated, $\tau_\alpha(h_j)$ is not initially parallel with g_k , so for the images to be initially parallel, the set $\alpha \cap g_k$ must be nonempty. Let $q \in \alpha \cap g_k$ be the intersection point closest to w_k (along g_k). There are two possibilities, depending on whether the orientations at α, h_j and at α, g_k agree (Figures 25(a),(d) indicate the two possibilities). For the case of Figure 25(a), the images $\tau_\alpha(h_j), \tau_\alpha(g_k)$ are initially parallel if and only if q, w_k are vertices in a downward triangle (Figure 25(b)), in which case they are completed by vertices v_{j+1}, w_{k+1} associated to v_j, w_k through the refining procedure (Figure 25(c)). For the case of Figure 25(d), the images are not initially parallel. Finally, note that this is all irrespective of any other intersection points $\alpha \cap h_j$ or $\alpha \cap g_k$.

For the case in which there is no isolated initial downward point, we proceed by first isotoping α into a ‘standard form’, from which the effect of the various types of intersection can be more easily determined. We require all intersection points to be either

- (1) in *crossing pairs* (p, q) such that (p, q) bounds a sub-arc of α whose interior lies entirely in the interior of either B or B' (Figure 26(a)), or
- (2) *diagonal*; i.e. a vertex of an upward triangle in the triple (α, γ_1, g_k) or (α, γ_2, h_j) (Figure 26(b)). Intuitively, this just means that α cuts off the upper-left or lower-right corner of B or B' .

Furthermore, we require that if T is an upward triangle with an endpoint (v_l or w_m) as a vertex, then there is a diagonal intersection point on $\alpha \cap T$ (Figure 28(b)). Note that if all intersection points can be put into crossing pairs, then this requirement ensures that the endpoints are not upward, and thus fixable. In this case the images are again initially parallel, along $\tau_\alpha(B)$, and completed, along

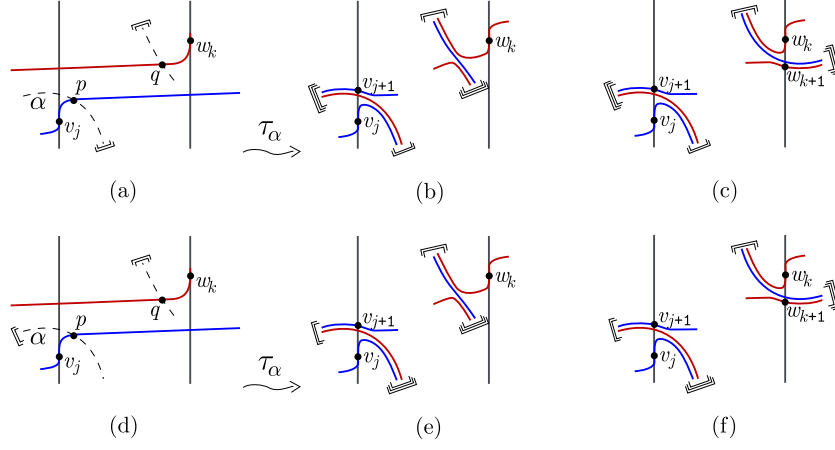


FIGURE 25.

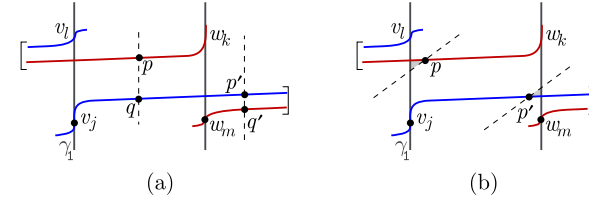


FIGURE 26. (a) p, q and p', q' are crossing pairs. (b) p, p' are diagonal.

$\tau_\alpha(B')$ (Figure 27). Recall that isotopies which cross either endpoint do not affect the images of the segments h_j, g_k under i_α , so the ‘standard position’ is easily attainable (Figure 28) by a sequence of shifts of α over the points v_l, w_m .

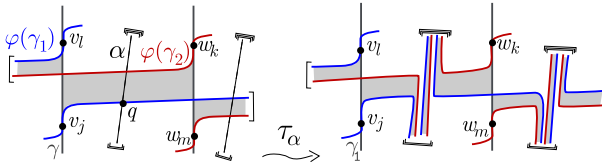


FIGURE 27. If all intersections are crossing pairs, and the endpoints fixable, then the images are again initially parallel, along $\tau_\alpha(B)$, and completed, along $\tau_\alpha(B')$.

We are left then with diagonal points. Suppose then that $p \in \alpha \cap h_j$ is diagonal. Following the argument of Lemma 3.18, the image $\tau_\alpha(h_j)$ can be initially parallel along $\tau_\alpha(\Delta)$ only if there are a pair of triangular regions in the triple $(\gamma_2, \varphi(\gamma_1), \alpha)$ with two points in common (one of them p), which by Lemma 3.17 determines the situation, illustrated in Figure 30(a). The only ambiguity concerns the relative position of the point w_m . Figures 30(b)-(d) illustrate the argument for one possibility, Figures 30(e)-(g) for the other.

□

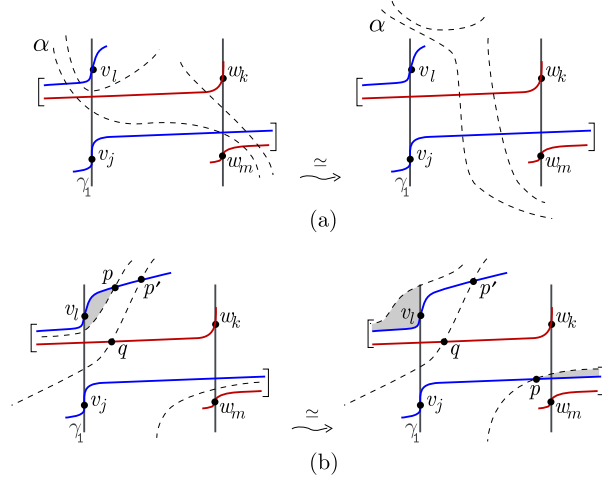


FIGURE 28. (a) Standard position for downward intersections. α is isotoped via shifts over the endpoints v_l, w_m so as to intersect B entirely in crossing pairs. (b) The points p, p' are upward intersections. The upward triangle T for p is shaded. Note that, before the isotopy, $\alpha \cap T$ contains no diagonal point of intersection, so α must be isotoped over v_l as indicated. The point q is neither upward nor downward.

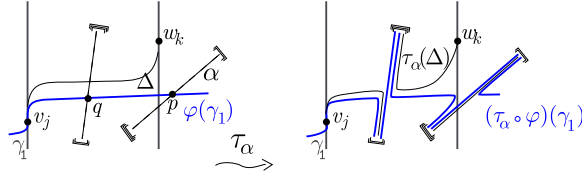


FIGURE 29. p is a diagonal intersection point. If p is not upward, there are no bigons in the image and so $\tau_\alpha(h_j)$ cannot be initially parallel along $\tau_\alpha(\Delta)$. However, as $\tau_\alpha(g_k)$ is to the right of $\tau_\alpha(\Delta)$ (at $i_\alpha(v_k)$), this implies that $\tau_\alpha(h_j), \tau_\alpha(g_k)$ are not initially parallel.

Finally, we bring all of the above together to prove Theorem 3.1.

Proof. (of Theorem 3.1) It follows from Lemmas 3.23, 3.26, and 3.27 that the inductive step of the algorithm preserves consistency of right positions. It is left to show that the base step, in which φ is a single twist τ_α , gives consistent right positions to each pair γ_1, γ_2 .

So, let \mathcal{P}_i be the right position associated to $(\gamma_i, \tau_\alpha(\gamma_i))$, $i = 1, 2$ by the base step. Suppose then that $h_j \in H(\mathcal{P}_1), g_k \in H(\mathcal{P}_2)$ are initially parallel horizontal segments, along disc B (Figure 31(a)). As noted in the construction of the base step, each $h_{i,i+1}$ is just the image of a segment of γ_1 which has a single intersection with α , with endpoints corresponding to each connected component of the fixable points $\gamma_1 \setminus \text{support}(\tau_\alpha)$, and similarly for each $g_{i,i+1}$. Thus, if n is the number of points of $\mathcal{P}_1 \cap \partial B$, then h_j, g_k are completed by the points v_{j+n+1}, w_{k+n+1} . Figure 31(b) illustrates the local picture for the case $n = 1$.

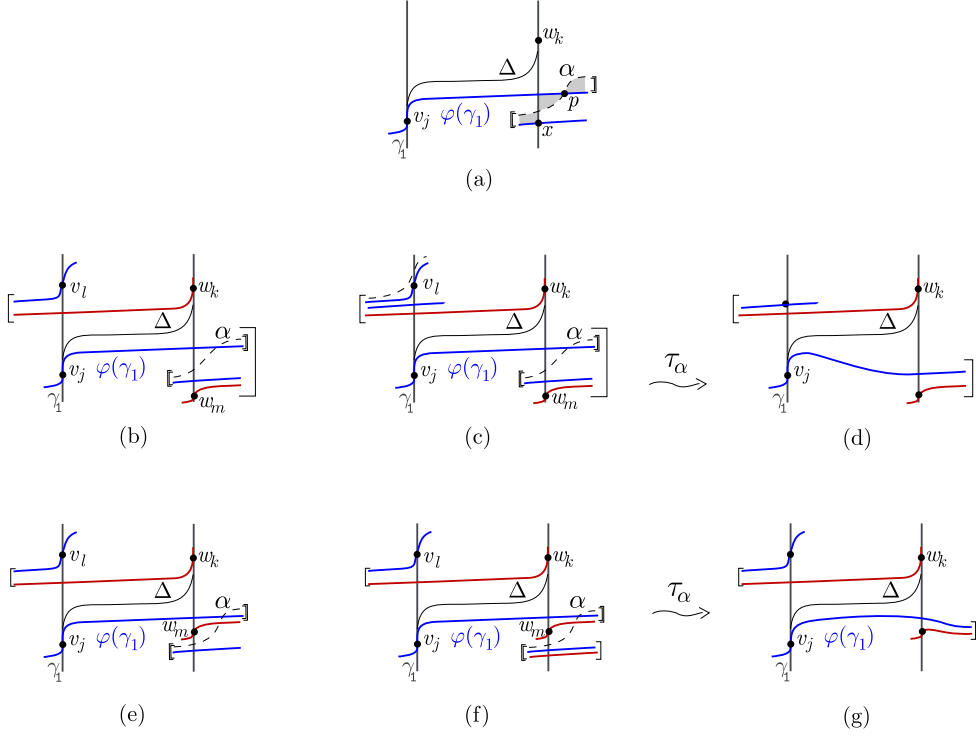


FIGURE 30. (a) If $\alpha \cap h_j$ is a diagonal intersection point p , then $\tau_\alpha(h_j)$ can be initially parallel along $\tau_\alpha(\Delta)$ only if the image $\tau_\alpha(h_j)$ and γ_2 bound canceling bigons, corresponding to the shaded triangular regions. (b) The case that w_m is ‘below’ x . (c) indicates the relevant features of the configuration determined by the situation, and (d) shows the image, which is completed. (e),(f) and (g) do the same for the case w_m is ‘above’ x .

By induction, then, given a surface Σ , and $\varphi \in \Gamma_\Sigma$ with positive factorization ω , the associated right positions $\mathcal{P}_\omega(\gamma)$, $\mathcal{P}_\omega(\gamma')$ are consistent for any nonintersecting properly embedded arcs γ, γ' . \square

4. RESTRICTIONS ON $p.e.(\varphi)$

In this section, we switch focus back to the entirety of pairs of distinct properly embedded arcs γ_1, γ_2 in a surface Σ , and the images of these arcs under right-veering $\varphi \in \Gamma_\Sigma$. The motivating observation here is that, as the endpoints of each arc are by definition included in any right position, the property of h_0, g_0 being initially parallel is independent of right position, and so is a property of the pair $\varphi(\gamma_1), \varphi(\gamma_2)$. In particular, for *positive* φ , if $\varphi(\gamma_1), \varphi(\gamma_2)$ are initially parallel, they must admit consistent right positions $\mathcal{P}_i(\varphi, \gamma_i)$ in which the initial segments are completed (see Example 3.7). We are interested in understanding what necessary conditions on $\alpha \in p.e.(\varphi)$ (Definition 2.1) can be derived from the information that $\varphi(\gamma_1), \varphi(\gamma_2)$ are initially parallel. These are summarized in Lemmas 4.4 and 4.10.

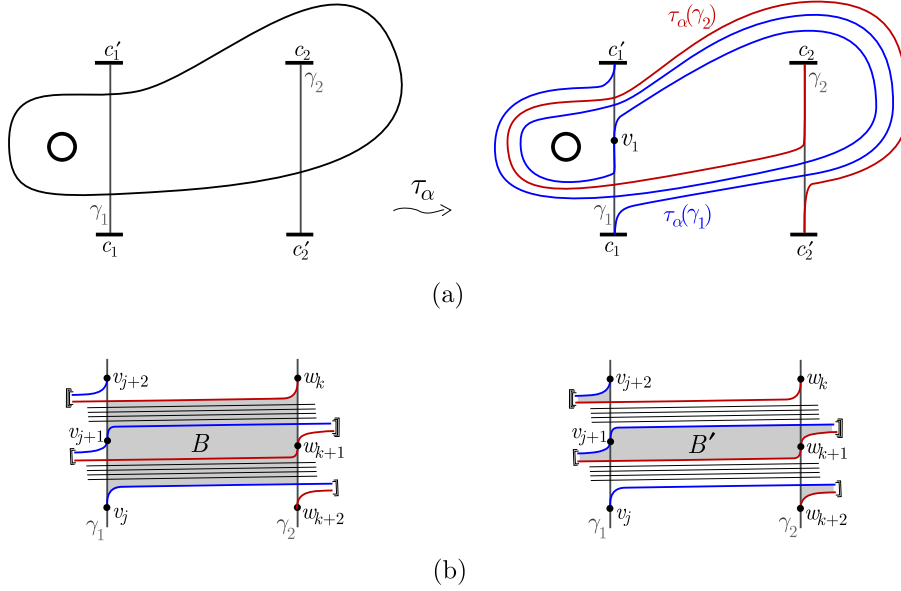


FIGURE 31. (a) An example of the right position associated to a single Dehn twist. (b) Initially parallel h_j, g_k are completed by v_{j+2}, w_{k+2}

Throughout the section, we will be considering embedded rectangular regions $R \hookrightarrow \Sigma$, and classifying various curves and arcs by their intersection with such regions. We need:

Definition 4.1. Let R be a rectangular region with distinguished oriented edge e_1 , which we call the base of R . We label the remaining edges e_2, e_3, e_4 in order, using the orientation on e_1 (Figure 32). We classify properly embedded (unoriented) arcs on R by the indices of the edges corresponding to their boundary points, so that an arc with endpoints on e_i, e_j is of type $[i, j]$ (on R). We are only concerned with arcs whose endpoints are not on a single edge. An arc on R is then

- horizontal if of type $[2, 4]$
- vertical if of type $[1, 3]$
- upward if of type $[1, 2]$ or $[3, 4]$
- downward if of type $[1, 4]$ or $[2, 3]$
- non-diagonal if horizontal or vertical
- type 1 if not downward

Definition 4.2. Let $R \hookrightarrow \Sigma$ be an embedded rectangular region with distinguished base as in Definition 4.1. We say $\alpha \in SCC(\Sigma)$ is type 1 on R if each arc $\alpha \cap R$ is type 1 on R .

Following Definition 4.1, we use a given pair of properly embedded arcs to define a rectangular region $D \hookrightarrow \Sigma$ as follows: Suppose γ_1, γ_2 are disjoint properly embedded arcs, where $\partial\gamma_i = \{c_i, c_i'\}$, and $\tilde{\gamma}_1$ is a given properly embedded arc with endpoints c_1', c_2 . Let $\tilde{\gamma}_2$ be a parallel copy of $\tilde{\gamma}_1$ with endpoints isotoped along γ_1, γ_2 to c_1, c_2' . We then define $D \hookrightarrow \Sigma$ as the rectangular region bounded by $\gamma_1, \gamma_2, \tilde{\gamma}_1, \tilde{\gamma}_2$

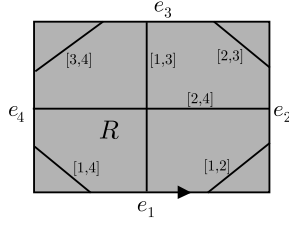


FIGURE 32. Representatives of each of the 6 possible types of arc on R

(the endpoints are labeled so that c_1 and c_2 are diagonally opposite), and base $\bar{\gamma}_2$, oriented away from c_1 (see Figure 33). For the remainder of this section, D will always refer to this construction. Of course, for a given pair of arcs, D is unique only up to the choice of $\bar{\gamma}_1$. We also make use of the *diagonal* Δ of D , a representative of the unique isotopy class of arcs with boundary $\{c_1, c_2\}$ and interior within D . In particular, the diagonal determines $\bar{\gamma}_1$, and vice versa.

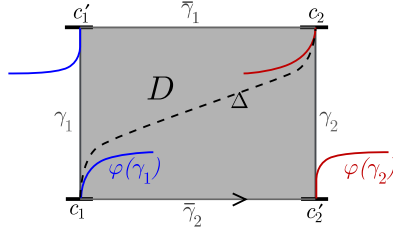


FIGURE 33. disc construction

Definition 4.3. We say the pair $\varphi(\gamma_1), \varphi(\gamma_2)$ is flat if D can be constructed such that $\varphi(\gamma_i) \cap \bar{\gamma}_j = \emptyset$ for $i, j \in \{1, 2\}$, and initially parallel (on D) if there exists D such that $\varphi(\gamma_1), \varphi(\gamma_2), \gamma_1, \gamma_2$ bound a disc $B \leftrightarrow D$ on which c_1, c_2 are vertices.

As expected, then, the pair of arcs $\varphi(\gamma_1), \varphi(\gamma_2)$ is initially parallel exactly when the horizontal segments h_0, g_0 of each pair of right positions are initially parallel. Using this, we immediately obtain:

Lemma 4.4. Let φ be positive, and $\varphi(\gamma_1), \varphi(\gamma_2)$ initially parallel on D . Then $\alpha \in p.e.(\varphi)$ only if α is type 1 on D .

Proof. Suppose otherwise - then $\alpha \cap D$ has an arc of type $[1, 4]$ or $[2, 3]$ on D . Now, if $\alpha \in p.e.(\varphi)$, there is some positive factorization of φ in which τ_α is the initial Dehn twist. However, if $\alpha \cap D$ has an arc of type $[1, 4]$, then $\tau_\alpha(\gamma_1)$ is strictly to the right of $\varphi(\gamma_1)$ (in the sense of section 2), while if the arc is of type $[2, 3]$, then $\tau_\alpha(\gamma_2)$ is strictly to the right of $\varphi(\gamma_2)$, either of which contradicts $\varphi(\gamma_1), \varphi(\gamma_2)$ being initially parallel. \square

To tie this more firmly to the previous section, note that, by Theorem 3.1, if φ is positive, there are consistent right positions $\mathcal{P}_1, \mathcal{P}_2$ for any pair $\varphi(\gamma_1), \varphi(\gamma_2)$. Now, if the initial horizontal segments $h_0 \in H(\mathcal{P}_1), g_0 \in H(\mathcal{P}_2)$ are initially parallel, then

there are unique $v \in \mathcal{P}_1, w \in \mathcal{P}_2$ such that v, w are endpoints of the completed segments. Letting B' be the completing disk (Definition 3.5), we can define a new disc by extending B' so that its corners lie on $\bar{\gamma}_i$, rather than γ_i :

Definition 4.5. A bounded path in (Σ, D, φ) is a rectangular region $P \hookrightarrow \Sigma$ bounded by $\bar{\gamma}_i, \varphi(\gamma_i), i = 1, 2$, with corners c_1, c_2 in common with D (Figure 34).

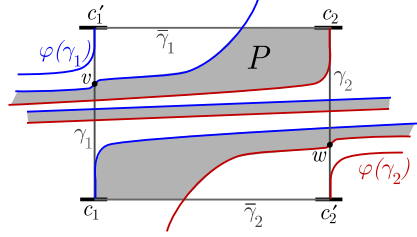


FIGURE 34. P is a bounded path for type 1 $\varphi(\gamma_1), \varphi(\gamma_2)$.

Lemma 4.6. If $\varphi(\gamma_1), \varphi(\gamma_2)$ is initially parallel, for positive φ , then (Σ, D, φ) has a bounded path.

Proof. This is a restatement of the above discussion. □

Let Σ, D , and φ be given such that the pair $\varphi(\gamma_1), \varphi(\gamma_2)$ is initially parallel and flat (and thus initially parallel) with respect to D . The remainder of this section is an exploration of what necessary conditions this places on elements of $p.e.(\varphi)$.

We start by observing that under these conditions (i.e. initially parallel and flat), the pair of trivial right positions whose vertical sets consist only of the arc boundary points are consistent. Also, the entirety of each image $\varphi(\gamma_i)$ is in the boundary of the bounded path (see Figure 35). In particular, such images are *parallel* in the sense of Definition 2.4. Now, for $\alpha \in SCC(\Sigma)$, it is clear that α is flat (i.e. $\alpha \cap \bar{\gamma}_1 = \alpha \cap \bar{\gamma}_2 = \emptyset$) if and only if all arcs $\alpha \cap P$ are horizontal on P (Definition 4.1), and that, for such curves, $(D, \tau_\alpha^{-1}\varphi)$ is again initially parallel and flat, and so admits consistent right positions. Our interest then lies in non-flat α .

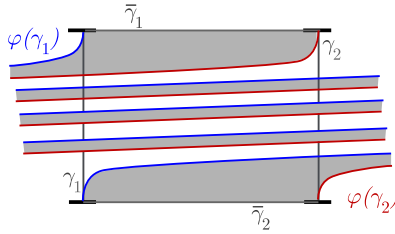


FIGURE 35. The bounded path of flat, initially parallel (D, φ)

Lemma 4.7. Let $\varphi(\gamma_1), \varphi(\gamma_2)$ be flat and initially parallel. Then $\alpha \in p.e.(\varphi)$ only if:

- (1): $\alpha \cap \gamma_1 \neq \emptyset \Leftrightarrow \alpha \cap \gamma_2 \neq \emptyset$
- (2): $\alpha \cap \varphi(\gamma_1) \neq \emptyset \Leftrightarrow \alpha \cap \varphi(\gamma_2) \neq \emptyset$

Proof. For statement (1), suppose α is such that $\alpha \cap \gamma_1 \neq \emptyset, \alpha \cap \gamma_2 = \emptyset$. Referring to Figure 32, this means that arcs $\alpha \cap D$ cannot be of type [2, 3], [1, 2] or [2, 4] on D , while any arc of type [1, 4] on D would result in $\tau_\alpha^{-1} \circ \varphi$ not being right veering. Similarly, arcs $\alpha \cap P$ cannot be of type [1, 2] or [1, 3] on P , while the right veering conditions eliminates [3, 4] and [1, 4]. Putting these together, we find that α may be isotoped such that all intersections $\alpha \cap P, D$ are along subarcs isotopic to one of the ρ, ρ', ρ'' shown in the left side of Figure 37, and in particular that there is at least one along ρ .

Now, for such α , the pair $\tau_\alpha^{-1}(\varphi(\gamma_1)), \tau_\alpha^{-1}(\varphi(\gamma_2))$ is initially parallel, and so, if $(\tau_\alpha^{-1} \circ \varphi)$ is positive, must contain a bounded path. Also, arcs along ρ', ρ'' preserve the bounded path (are ‘cutting pairs’ in the sense of Lemma 3.27), so we may assume all intersections are along ρ . (Figure 36). It is immediate then that $(D, \tau_\alpha^{-1}\varphi)$ has no bounded path.

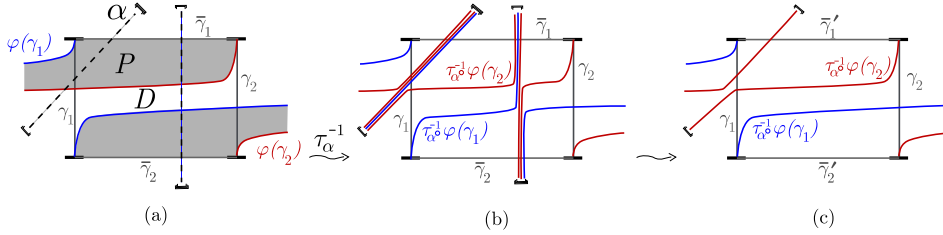


FIGURE 36. Illustration of the terminology of Lemma 4.7. (a) A typical α , with a ‘cutting pair’ of intersections, and a diagonal intersection. (b) is the image under τ_α^{-1} . Notice that, to recover a standard picture of the associated D , we must ‘normalize’ the picture as in (c), thereby justifying the assertion that ‘cutting pairs may be ignored’. It is clear that there is no bounded path.

The argument for statement (2) is nearly identical: We suppose $\alpha \cap \varphi(\gamma_1) \neq \emptyset, \alpha \cap \varphi(\gamma_2) = \emptyset$, and find that all intersections $\alpha \cap P, D$ are isotopic to one of the arcs $\sigma, \sigma', \sigma''$ shown in the right side of Figure 37, and in particular that there is at least one along σ . Again, $(D, \tau_\alpha^{-1}\varphi)$ has no bounded path.

Note that this is a slight generalization of the second example of Example 3.7.

□

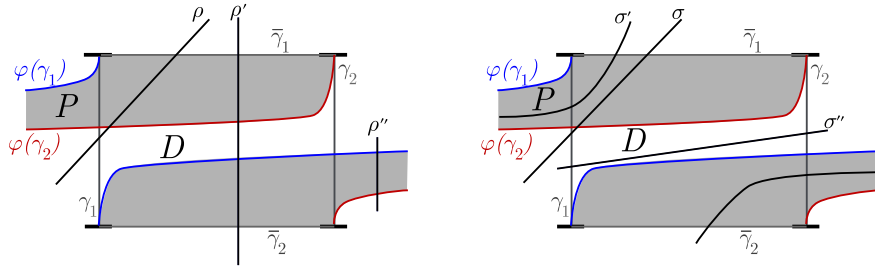


FIGURE 37.

We have one final application of the bounded path construction. Note that, for α, D as above, an orientation of α gives a derived orientation on each arc in $D \cap \alpha$. Thus, given a pair of upward arcs, we can ask whether their derived orientations agree, independently of the actual orientation of α .

Lemma 4.8. *Let $\varphi(\gamma_1), \varphi(\gamma_2)$ be flat and initially parallel. Let α be type 1 on D , such that $\alpha \cap D$ has exactly 2 diagonal arcs s_1, s_2 . Then $\alpha \in p.e.(\varphi)$ only if the derived orientations on s_1 and s_2 agree.*

Proof. Note firstly that, by Lemma 4.7, s_1, s_2 must be as in Figure 38(a); i.e. one cuts the upper left corner of D , the other the lower right corner. We show that $(D, \tau_\alpha^{-1}\varphi)$ has a bounded path if and only if the derived orientations on s_1, s_2 agree, which, by Lemma 4.6 gives the result.

Note that if $\alpha \cap D$ has a horizontal arc, it cannot have a vertical arc, and vice-versa. We distinguish the two cases:

- (1) $\alpha \cap D$ has no vertical arcs. The boundary of bounded path P must include the initial segments of each arc $\tau_\alpha^{-1}(\varphi(\gamma_i))$ from $c_i, i = 1, 2$. We can then start from either corner c_i and follow the initial segment around α . Figure 38 does this for c_1 . It is clear then that these initial segments will close up to bound P if the orientations match (Figure 38(b)). If, on the other hand, the orientations do not match, the segments do not form the boundary of a bounded path (Figure 38(c)).
- (2) $\alpha \cap D$ has no horizontal strands. If there are vertical strands, we must adjust D such that the diagonal is given by $\tau_\alpha^{-1}(\Delta)$. Again, as in case (1), there is a bounded path if and only if the derived orientations on s_1 and s_2 agree.

□

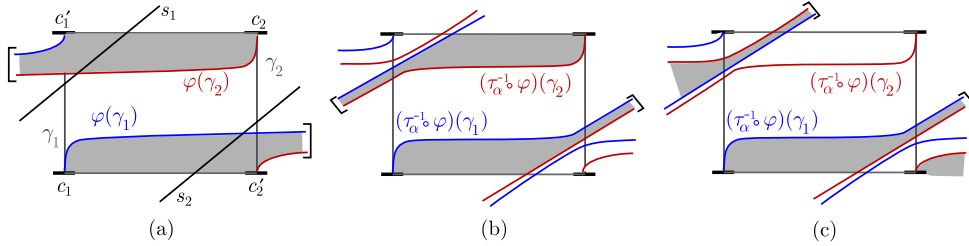


FIGURE 38. (a) $\alpha \cap D$ has exactly 2 diagonal arcs s_1, s_2 . (b) Orientations agree. (c) Orientations disagree.

To sum up, for flat (D, φ) , $\alpha \in p.e.(\varphi)$ only if α is type 1 on D , and satisfies the intersection conditions of Lemma 4.7. Furthermore, if $\alpha \cap D$ has only two diagonal arcs, it must satisfy the orientation conditions of Lemma 4.8. We now wish to utilize the results of Section 3 to extend these results to the horizontal segments of consistent right positions of the arc/monodromy pairs, and thus to obtain stronger necessary conditions on arbitrary type 1 α for inclusion in $p.e.(\varphi)$.

Given (D, φ) , and a type 1 curve α , we label the upward sloping arcs $s_i \in \alpha \cap D$ as in Figure 39. A subarc s_i is thus defined only in a neighborhood of the point x_i . Let a_1, a_2, \dots, a_m , where $a_1 = 1, m = \max\{m_1, m_2\}$, be the indices of the x_i

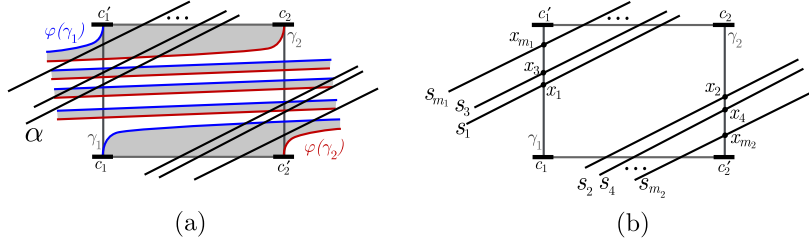


FIGURE 39. (a) The diagonal arcs of $\alpha \cap D$. (b) Labeling of arcs and intersections.

with order given by the order in which they are encountered traveling along α to the right from $x_1 \cap \gamma_1$. We associate to α the list $\pi_\alpha = (a_1, a_2, \dots, a_m)$, defined up to cyclic permutation. We decorate these entries with a bar, \bar{a}_j , if the derived orientations of s_{a_j} and s_1 do not agree.

Definition 4.9. We say α is nested with respect to D if its associated π_α can be reduced to the trivial by successive removals of pairs $(i, i+1)$ or $(i+1, i)$ of consecutive entries, i odd, and balanced if the derived orientations of each such pair agree.

For example, $(\bar{14}5632)$ is nested but not balanced, (135462) is balanced but not nested, and $(\bar{14}56\bar{3}2)$ is both nested and balanced. Note that either definition requires π_α to have even length. The motivation for these definitions becomes clear with the following:

Theorem 4.10. Let (D, φ) be flat and parallel. Then $\alpha \in p.e.(\varphi)$ only if α is nested and balanced with respect to D .

We will postpone the proof so as to introduce terminology and a couple of helpful lemmas. The basis of the argument is that, if $\alpha \in p.e.(\varphi)$, then $\tau_\alpha^{-1} \circ \varphi$ admits a positive factorization, and so by Theorem 3.1 there are consistent right positions \mathcal{P}_i of $\tau_\alpha^{-1}(\varphi(\gamma_i))$. By Lemma 4.6 the arcs $\tau_\alpha^{-1}(\varphi(\gamma_i))$ are initially parallel, and so the \mathcal{P}_i must include the uniquely determined completing points v_1, w_1 . We show by induction that, for $j \geq 1$, each pair of horizontal segments h_j, g_j , is also initially parallel, and so each pair v_{j+1}, w_{j+1} is uniquely determined in a way that requires π_α balanced for compatibility of the pairs h_j, g_j , and nested for overall consistency of the right positions.

We begin by using D to define a sequence of decompositions of α into pairs of arcs. We refer to Figure 39 for notation. Let π_α be as in the paragraph preceding Definition 4.9, give α the orientation in which s_1 is directed from γ_1 to $\bar{\gamma}_1$, and, using this orientation, denote the sub-arc of α from x_i to x_j by $[x_i \dots x_j]$, including the endpoints, or $(x_i \dots x_j)$ not including the endpoints. We then define $\rho_i := [x_{2i+2} \dots x_{2i+1}]$ and $\sigma_i = (x_{2i-1} \dots x_{2i})$. Each pair ρ_i, σ_{i+1} thus decomposes α into two arcs.

We further label the diagram by, in each neighborhood of x_i , labeling each of the m s_i -parallel segments of $\tau_\alpha^{-1}(\varphi(\gamma_j))$ by $s_i^{b_1}, \dots, s_i^{b_m}$, where s_i^j is the sub-arc of $[y_j, y_{j+2}]$ along s_i . In particular, $b_m = i$, and $(b_1 \dots b_m) = \pi_\alpha$ up to cyclic permutation and reversal (see Figure 40). Again, this labeling system is only valid in the image (under τ_α^{-1}) of a neighborhood of x_i .

Referring to Figure 40, we see that the path of $\tau_\alpha^{-1}(\varphi(\gamma_i))$ from $c_i \in \partial(\Sigma)$ is given by firstly following the diagonal Δ (we have drawn the case in which $\alpha \cap D$ has no vertical strands - in general, of course, Δ itself will go around α once for every vertical strand), and then going m times around α , after which it continues as in $\varphi(\gamma_i)$. We break the initial part of $\tau_\alpha^{-1}(\varphi(\gamma_1))$ into consecutive sub-arcs $[c_1, y_2], [y_2, y_4], \dots, [y_m, y_{m+2}]$, where $[c_1, y_2]$ follows Δ , while each $[y_i, y_{i+2}]$ follows the paths $\rho_{\frac{i}{2}-1}$ and then $\sigma_{i/2}$. Likewise, replacing c_1 with c_2 , and y_i with y_{i-1} , the arc $(\tau_\alpha^{-1} \circ \varphi)(\gamma_2)$ has the same decomposition, but following each sub-arc in the opposite direction.

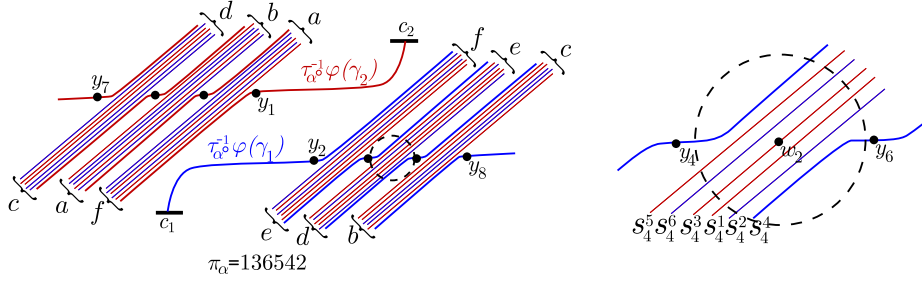


FIGURE 40. $\tau_\alpha^{-1}(\varphi(\gamma_i))$, for α with $\pi_\alpha = 136542$ (strands terminating in brackets with like letters are meant to be identified) and a detail of a neighborhood of the image under τ_α^{-1} of $s_4 \cap \varphi(\gamma_1)$

Lemma 4.11. *Let α be balanced with respect to flat, parallel (D, φ) . Then there are unique right positions \mathcal{P}_i^* for $(\gamma_i, \tau_\alpha^{-1}(\varphi(\gamma_i)))$, $i = 1, 2$ which satisfy the following:*

- (1) *If \mathcal{P}_i are any pair of consistent positions for $(\gamma_i, \tau_\alpha^{-1}(\varphi(\gamma_i)))$, then $\mathcal{P}_i^* \subset \mathcal{P}_i$ for each i , and*
- (2) *Each pair $h_j \in \mathcal{P}_1^*, g_j \in \mathcal{P}_2^*$ is initially parallel, and completed by v_{j+1}, w_{j+1} .*

Proof. The initial segments h_0, g_0 are initially parallel along Δ , after which they continue along ρ_0 to the points $v_1 := s_1^2 \cap \gamma_1$, $w_1 := s_2^1 \cap \gamma_2$. As s_1, s_2 have the same derived orientation, the initial segments h_0, g_0 are completed by v_1, w_1 (this is implicit in Lemma 4.7).

The segments h_1, g_1 are then initially parallel along σ_1 (because σ_j is simply $\alpha \setminus \rho_{j-1}$), and will then continue along ρ_1 to the points $v_2 := s_3^4 \cap \gamma_1$, $w_2 := s_4^3 \cap \gamma_2$. Note that these will be positive intersection points if and only if the arcs s_3, s_4 have the same orientation (which they do, as we are assuming α balanced), in which case they are completing points for h_1, g_1 . To satisfy condition (1), we add them to \mathcal{P}_i^* . We continue inductively to obtain the desired positions \mathcal{P}_i^* . The interior points of \mathcal{P}_1^* are thus $\{s_{i-1}^{2i} \cap \gamma_1\}$, and interior points of \mathcal{P}_2^* are $\{w_i := s_{2i}^{2i-1} \cap \gamma_1\}$. Using the above notation, for each j , the segments h_j, g_j are initially parallel along σ_j , and completed along ρ_j . □

We are now ready to prove Theorem 4.10. We break the statement into two lemmas, starting with:

Lemma 4.12. *Let (D, φ) be flat and parallel. Then $\alpha \in p.e.(\varphi)$ only if α is balanced with respect to D .*

Proof. Suppose α is *not* balanced with respect to D . By Lemma 4.7, we may assume that, for $i = 1, 2$, there is at least one upward arc of $\alpha \cap D$ with endpoint γ_i . To keep notation manageable, we start with the case that the ‘initial’ pair s_1, s_2 derive opposite orientations, and then use Lemma 4.11 to adapt the argument for the general case. Now, if there are no other arcs, this is just Lemma 4.8. The proof here is similar, in that we follow along the initially parallel segments h_0 and g_0 and show that they cannot be completed.

Note that the entire image is determined by the ‘local pictures’ given by the images (under τ_α^{-1}) of the neighborhoods of points $\alpha \cap \gamma_i$ and the information of how they fit together (as in Figure 40). So as to avoid repeating the phrase, we will refer to “the image (under τ_α^{-1}) of the neighborhood of $s_j \cap \gamma_i$ ” simply as N_j (note that the index i is determined by parity of j , so extraneous).

Consider then the neighborhood N_1 (the relevant segments of N_1 and N_2 are illustrated in Figure 41(a)). If the pair h_0, g_0 are completed, then the arcs s_1^2, s_1^1 must each be in the boundary of the completing disc B' , but as the orientations of these arcs do not match, the completing endpoint v_1 must lie on some other arc s_1^j (Figure 41(b)). As B' is embedded, s_1^j must lie between s_1^2, s_1^1 . In particular, this means that the entire segment of h_0 up to the point y_{2j+2} must lie in $\partial B'$. For our purposes, it is enough to notice that the point y_4 must lie in $\partial B'$.

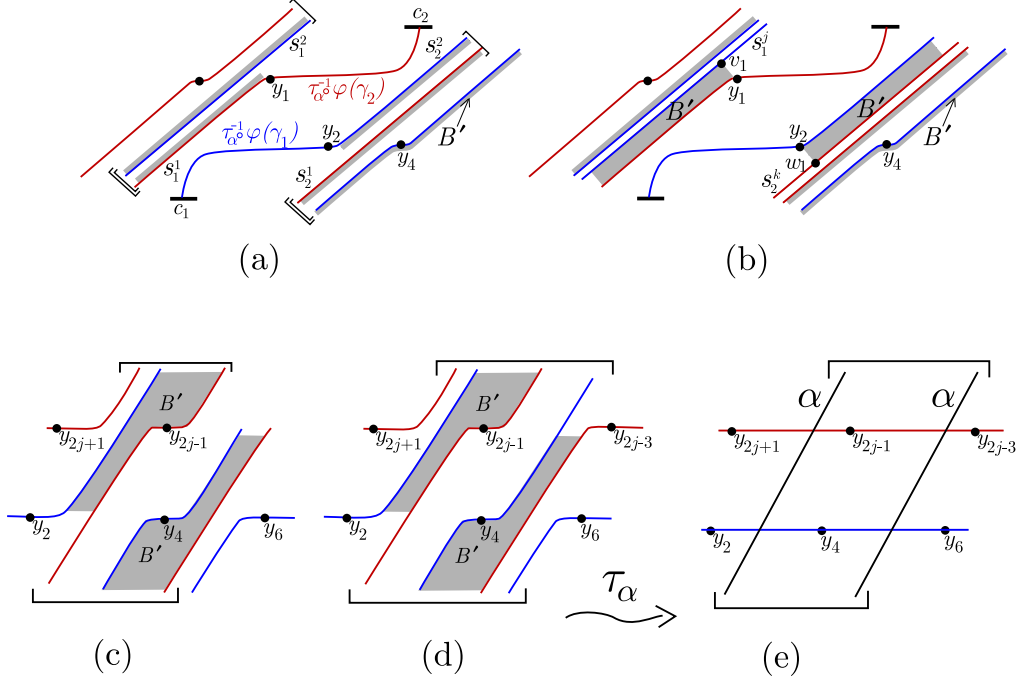


FIGURE 41. Figures for Lemma 4.12

The trick is then to use this information to piece together relevant neighborhoods. We start in N_2 (Figure 41(c)). By an identical argument to that of the previous paragraph, there is an arc s_2^k , lying between s_2^2 and s_2^1 , such that w_1 is on s_2^k . Now, as $\partial B'$ must extend along h_0 up to y_4 , the neighborhood N_k is encountered as

we follow B' from N_2 to N_4 . This gives up the necessary information to follow B' through the neighborhoods N_2, N_4, N_k, N_{k-2} (Figure 41(d)). However, these neighborhoods can connect with this pattern only if α is not connected (Figure 41(e)), a contradiction.

For the general case, let $l-1$ be the smallest (even) index such that the $\{s_i\}, i < l$ are all balanced. Now, by Lemma 4.11, if $(\gamma_i, (\tau_\alpha^{-1} \circ \varphi)(\gamma_i))$ have consistent positions \mathcal{P}_i , then \mathcal{P}_1 must contain the points $\{s_{j-1}^{2j} \cap \gamma_1\}, 1 \leq j \leq l$, and likewise \mathcal{P}_2 must contain $\{w_i := s_{2j}^{2j-1} \cap \gamma_1\}, 1 \leq j \leq l$. Furthermore, h_l, g_l are initially parallel along σ_l .

To violate the balanced condition, either:

- (1) s_l, s_{l+1} derive opposite orientations. The proof goes through exactly as above, replacing h_0, g_0 with h_l, g_l , and each N_i with N_{2i+2} . The segments h_l, g_l are not completed. or
- (2) There is arc s_l , but no corresponding s_{l+1} (or vice versa). As the points $\{v_i\}, \{w_i\}$ are determined, this is just a localized version of Lemma 4.7. In particular, the completing endpoint for g_l must be the endpoint c'_2 , but this does not give a completing disc. Figure 42 shows the relevant discs.

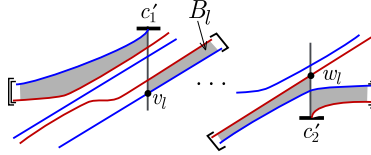


FIGURE 42.

In each case $(\gamma_i, \tau_\alpha^{-1}(\varphi(\gamma_i)))$ admit no consistent right positions, and so α cannot be in $p.e.(\varphi)$. □

Finally, the proof of Theorem 4.10 is completed by:

Lemma 4.13. *Let (D, φ) be flat and parallel. Then $\alpha \in p.e.(\varphi)$ only if α is nested with respect to D .*

Proof. Note firstly that, if there are at most 2 diagonal arcs in $\alpha \cap D$, this is exactly Lemmas 4.7 and 4.8. For, by Lemma 4.7, π_α of such a curve must be one of $\{(1, 2), (1, \bar{2})\}$ (so α is trivially nested), and so by Lemma 4.8, we must have $\pi_\alpha = (1, 2)$, i.e. α is balanced.

By Lemmas 4.11 and 4.12, it suffices to show that the unique positions \mathcal{P}_i^* , $i = 1, 2$, are consistent only if α is nested. In particular, for balanced α , each pair $h_j \in H(\mathcal{P}_1^*), g_j \in H(\mathcal{P}_2^*)$ is initially parallel and completed. We will show that the ‘mixed’ pairs $h_j, g_k, j \neq k$, satisfy the consistency conditions only if π_α is nested.

Suppose then that α is not nested. So, by Definition 4.9 there is some j, k (we take $j < k$) such that the sublist $\pi_{\sigma_j} = (2j - 1, \dots, 2j)$ of π_α contains $2k - 1$ but not $2k$, or contains $2k$ but not $2k - 1$ (we consider here only the first case - the proof for the second case is then obtained by switching v ’s and w ’s throughout). In our present context, we say π_{σ_j} overlaps π_{σ_k} in π_α .

Now, referring to the construction of the \mathcal{P}_i^* (Lemma 4.11), we can explicitly describe the strands s_m^l which make up the interior of the discs B_j, B'_j along which

h_j, g_j are initially parallel and completed:

$$\begin{aligned} \text{int}(B_j) &= \amalg_{l \in \text{int}(\pi_{\rho_{j-1}}), m \in \text{int}(\pi_{\sigma_j})} s_m^l \\ \text{int}(B'_j) &= \amalg_{l \in \text{int}(\pi_{\sigma_j}), m \in \text{int}(\pi_{\rho_{j-1}})} s_m^l \end{aligned}$$

The key observation here is that v_k is on the strand s_{2k-1}^{2k} , and so is in $\text{int}(B_j)$, and similarly $w_j \in \text{int}(B_k)$.

We pause for:

Lemma 4.14. *Let λ be a nested subword of π_α ; i.e. a consecutive list of entries in π_α which is nested. If $2k-1$ is an entry in λ , then the vertical points $v_k \in \mathcal{P}_1^*$, $w_k \in \mathcal{P}_2^*$ are not in the interior of any initially parallel disc B_j or completing disc B'_j .*

Proof. This is a direct consequence of the above calculations: an initially parallel disc B_j contains exactly the strands $\amalg_{l \in \text{int}(\pi_{\rho_{j-1}}), m \in \text{int}(\pi_{\sigma_j})} s_m^l$, while a vertical point v_k lies on s_{2k-1}^{2k} . So, if v_k is in the interior of B_j , we have $2k-1 \in \pi_{\sigma_j}$, and $2k \in \pi_{\rho_{j-1}}$. In particular, the entries $2j-1, 2k-1, 2j, 2k$ appear in that order in π_α , and so $2k-1$ is not in any nested subword. The argument for B'_j is identical. \square

We also require:

Observation 4.15. *Suppose γ_1, γ_2 is a right pair with consistent right positions $\mathcal{P}_1, \mathcal{P}_2$, with vertical points $v_j \in \mathcal{P}_1, w_k \in \mathcal{P}_2$. Let Σ' be the surface obtained by removal of a neighborhood of each of these points, and call the new boundary components ∂_v, ∂_w . Then, for $i = 1, 2$, let \mathcal{P}'_i be the restrictions of \mathcal{P}_i to the new arcs γ'_i , which follow the original arc from c_i to the respective new boundary component (Figure 43 makes this clear). It follows from Definition 3.6 that, if neither of v_j, w_k are in the interior of any initially parallel disc from the pair $\mathcal{P}_1, \mathcal{P}_2$, then $\mathcal{P}'_1, \mathcal{P}'_2$ are consistent.*

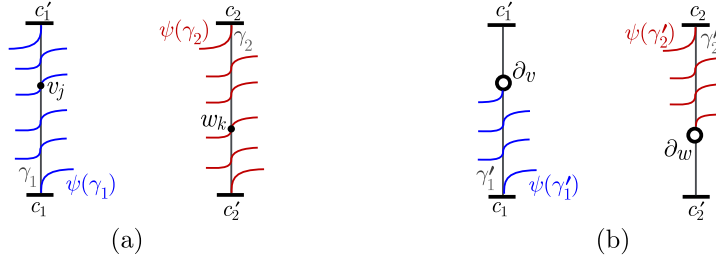


FIGURE 43. Construction of observation 4.15: (a) is the original configuration in Σ , (b) is the modified surface Σ'

We return to the proof of Lemma 4.13. Given non-nested π_α , let $2k-1$ be the largest entry such that $2k-1, 2k$ are not contained in a nested subword. Then by Lemma 4.14, v_{k+1}, w_{k+1} are not in the interior of any B_j, B'_j , and so using Observation 4.15, for the purposes of this proof, we may assume v_{k+1}, w_{k+1} are the endpoints c'_1, c'_2 ; i.e., $k = n$. So, w_j is in the interior of the intertwining disc B_n , and g_j is initially parallel with h_n (Figure 44). Let y be the corner of the initially parallel disc of h_n, g_j on $g_j \cap \gamma_1$. Now, if the pair is completed, there are endpoints

$v_l \in \mathcal{P}_1^{\alpha^{-1}}, w_m \in \mathcal{P}_2^{\alpha^{-1}}$. However, the completing disc (with corner w_m) terminates on γ_1 outside of B_n , and so cannot contain y , a contradiction.

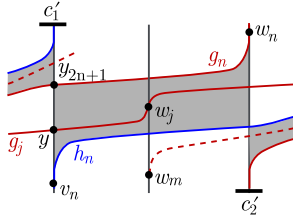


FIGURE 44. The initially parallel disc of the pair g_j, h_{n-1} lies in the interior of that of the compatible pair g_{n-1}, h_{n-1} . For completion of g_j, h_n , there must be endpoint w_m as indicated, but then the corresponding horizontal segment $g_{m,j}$, indicated by the dotted line, does not give a completing disc.

□

5. NON-POSITIVE OPEN BOOKS OF STEIN-FILLABLE CONTACT 3-FOLDS

In this section we prove Theorem 1.1 by constructing explicit examples of open book decompositions which support Stein fillable contact structures yet whose monodromies have no positive factorizations. We first introduce a construction, based on a modification of the lantern relation, which allows us to introduce essential left-twisting into a stabilization-equivalence class of open book decompositions. As, by Giroux, elements of such an equivalence class support a common contact manifold, proving the essentiality of this left-twisting (accomplished here using the methods of the previous sections) is sufficient to produce examples of non-positive open books which support Stein-fillable contact structures.

5.1. Immersed lanterns. For our construction, we start out using the usual lantern relation to give a mapping class equivalence between the words indicated in Figure 45(a) and (b), introducing a (non-essential) left twist about the curve α into a positive monodromy. We then stabilize by plumbing a positive Hopf band, use this stabilization curve to braid the lantern curves other than α into a new configuration in which the lantern relation does not apply, and then destabilize to a book in which, as the lantern is unavailable, the left twist about α has become essential. The steps are indicated clearly in the remainder of Figure 45. Note that to have room for the destabilization we must first enlarge the surface by adding a 1-handle (Figure 45(c)) to the support of the lantern relation, so that the associated open book decomposition is of $\#^2(S^1 \times S^2)$. This manifold is known to have a unique Stein-fillable structure, usually denoted ξ_{st} (recall that stabilization-equivalence to an open book with positive monodromy is sufficient to show Stein fillability of the supported contact manifold).

The remainder of this section uses the results of Section 4 to demonstrate that the left-twisting introduced by the ‘immersed lantern’ is in fact essential. We also show how this result generalizes to give similar examples of other open books with the same page.

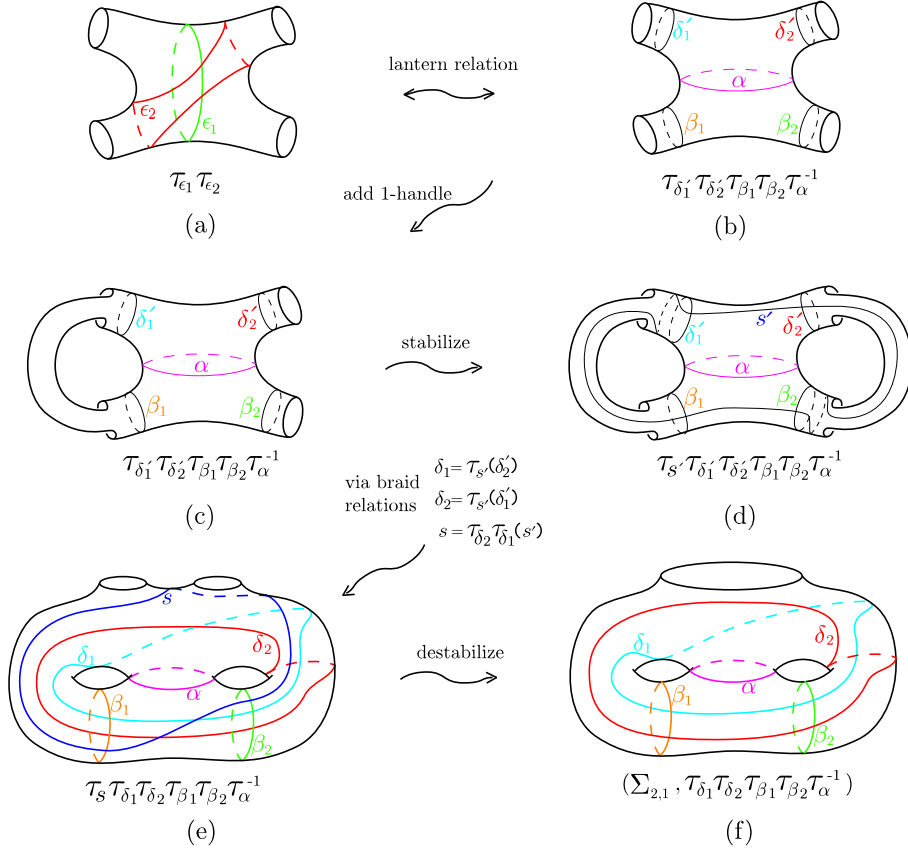


FIGURE 45. $(\#^2(S^1 \times S^2), \xi_{st}) = (\Sigma_{2,1}, \tau_\alpha^{-1} \tau_{\delta_1} \tau_{\delta_2} \tau_{\beta_1} \tau_{\beta_2})$.

5.2. The positive extension of φ' . Our method of demonstrating essentiality of the left twisting introduced by the immersed lantern is as follows: Let $\varphi = \tau_{\delta_1} \tau_{\delta_2} \tau_{\beta_1} \tau_{\beta_2} \tau_\alpha^{-1}$, where all curves are as in Figure 45, and define $\varphi' := \tau_\alpha \circ \varphi = \tau_{\delta_1} \tau_{\delta_2} \tau_{\beta_1} \tau_{\beta_2}$ (note that α has no intersection with any of the other curves, so τ_α commutes with each twist). Suppose that φ has positive factorization $\tau_{\alpha_n} \cdots \tau_{\alpha_1}$. Then we may factorize $\varphi' = \tau_\alpha \tau_{\alpha_n} \cdots \tau_{\alpha_1}$. Our goal is then to derive a contradiction by showing that $\alpha \notin p.e.(\varphi')$. This subsection comprises of two steps. Firstly, we show that α has trivial intersection with each curve in $p.e.(\varphi')$, and secondly use this to conclude that $\alpha \notin p.e.(\varphi')$. To put our figures more in line with those used in earlier sections, we consider the open book decomposition drawn in ‘almost planar’ form (Figure 46).

For the first step, we wish to show that $p.e.(\varphi')$ lies entirely on $\Sigma \setminus \alpha$ by applying the results of Section 4 to the pair γ_1, γ_2 shown in Figure 47. Observe firstly that $\Sigma \setminus \{\gamma_1, \gamma_2\}$ is a pair of pants bounded by β_1, β_2 , and α , and so these three curves are the only elements of $SCC(\Sigma)$ which have no intersection with $\{\gamma_1, \gamma_2\}$. The disc (D, φ') is flat (Definition 4.3), and so by the results of Section 4, and in particular Lemma 4.13, each curve $\epsilon \in p.e.(\varphi') \setminus \{\beta_1, \beta_2, \alpha\}$ is type 1, nested, and balanced. This brings us to:

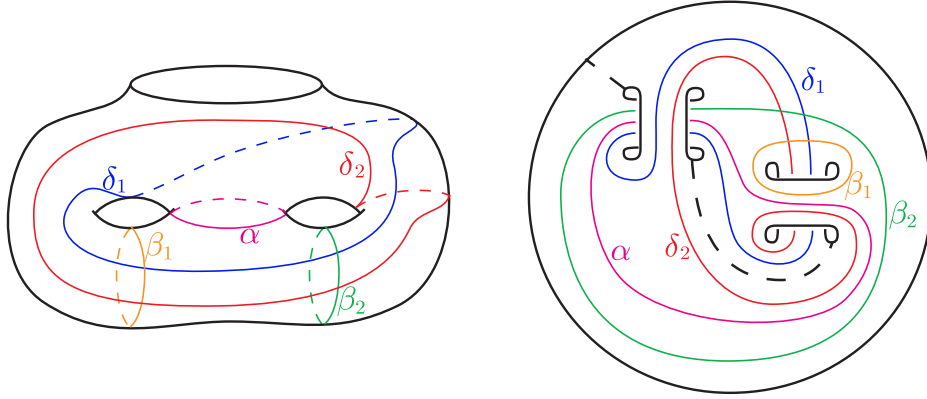


FIGURE 46. Two diagrams of $(\Sigma, \varphi) = (\Sigma_{2,1}, \tau_\alpha^{-1} \tau_{\delta_1} \tau_{\delta_2} \tau_{\beta_1} \tau_{\beta_2})$ - cutting the right figure along the dotted lines gives the equivalence.

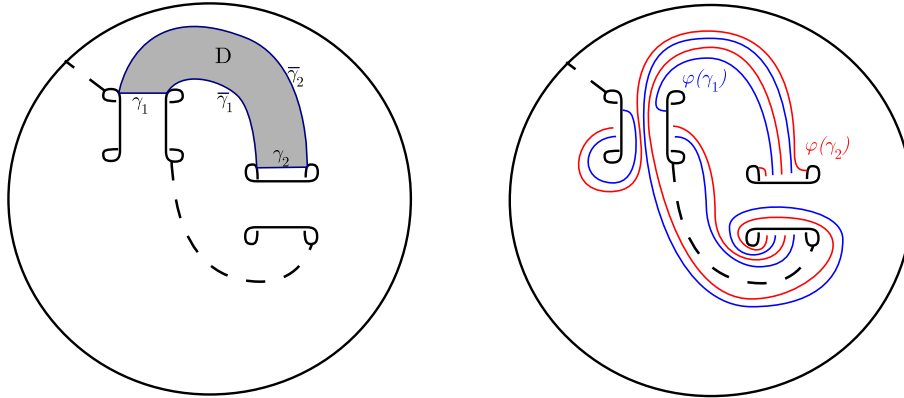


FIGURE 47. To the left, the arcs $\gamma_i, \tilde{\gamma}_i$, and the disc D . To the right, the images $\varphi'(\gamma_1), \varphi'(\gamma_2)$

Lemma 5.1. *Let Σ, α and D be as in Figures 46 and 47, and $\epsilon \in SCC(\Sigma)$ be type 1, nested, and balanced on D . Then $\epsilon \cap \alpha = \emptyset$*

Proof. We go through the proof for the case $\epsilon \cap D$ has no vertical segments (if this were not the case, then $\epsilon \cap D$ has no horizontal segments, and we would simply exchange γ_i and $\tilde{\gamma}_i$ throughout the proof).

Cut Σ along $\tilde{\gamma}_i, i = 1, 2$, keeping track of the points $\epsilon \cap \tilde{\gamma}_i$ (see Figure 48). The resulting surface is a pair of pants Σ' with points $\epsilon \cap \tilde{\gamma}_i$ labeled as in Figure 48, which are connected by m embedded, nonintersecting arcs $\epsilon \cap \Sigma'$. Further examples are given in Figure 49. Our goal is to show that none of these arcs intersect α .

Observe that these arcs correspond to pairs (i, j) of consecutive entries in π_ϵ (Definition 4.9), where i, j are the indices of the arc endpoints (so, e.g., if there is an arc with endpoints $\{p_4, r_3\}$, then 3, 4 appear consecutively in π_α in either order). We call an arc *paired* if its corresponding pair is of form $(i, i + i)$ or $(i + 1, i)$, for i odd. As ϵ is nested, $\epsilon \cap \Sigma'$ contains at least two paired arcs.

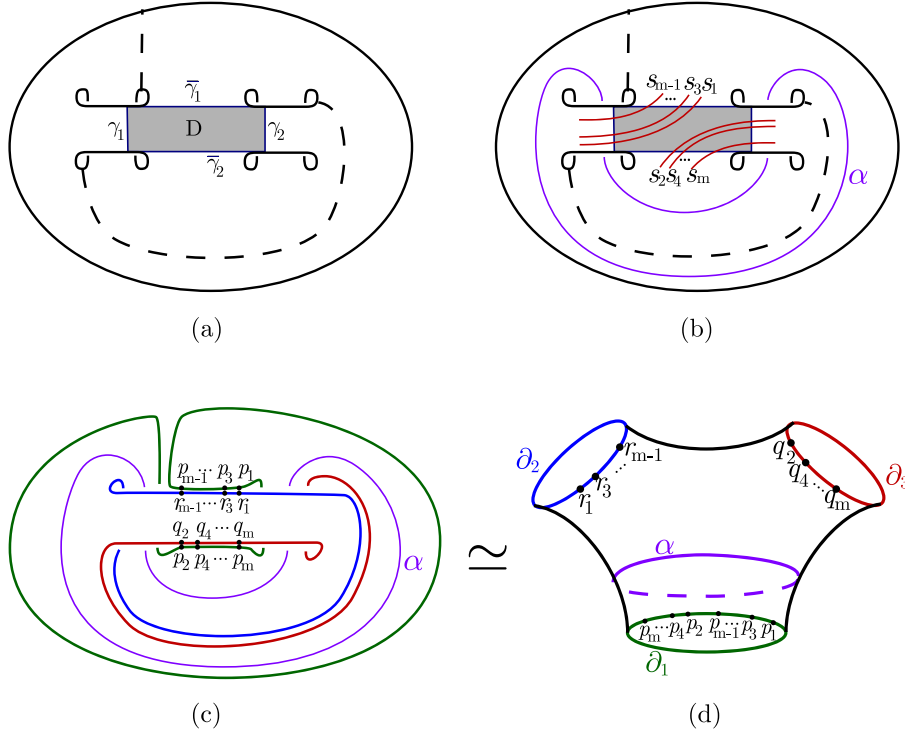


FIGURE 48. (a) indicates the disc D in Σ - again, Σ is obtained by cutting along the dotted lines. (b) shows the curve α , and diagonal arcs $\{s_i\} = \epsilon \cap D$ on Σ , while (c) and (d) illustrate the construction of Σ' by cutting Σ , and indicate the various boundary points used in the Lemma.

Referring again to Figure 48, we classify the arcs by the boundary components on which the endpoints lie. There are six possibilities, denoted $[p, p]$, $[q, q]$, $[r, r]$, $[r, q]$, $[p, r]$, or $[p, q]$. Furthermore, we see that if ϵ is balanced (Definition 4.9), then all *paired* arcs are of form $[p, p]$ or $[r, q]$.

We further distinguish arcs by the parity of the indices of their endpoints, along with the derived orientation of the corresponding arc s_i in $\epsilon \cap D$, which is already encoded in π_ϵ . In particular, we label an endpoint as type e if its index appears in π_ϵ as even or $\overline{\text{odd}}$, and type o if odd or $\overline{\text{even}}$.

Observe that a paired arc of form $[p, p]$ will separate ∂_1 such that no other paired arc can be of form $[p, p]$, so there is some paired $[r_i, q_{i+1}]$. Now, all other arcs must lie on the annulus $\Sigma'' := \Sigma' \setminus [r_i, q_{i+1}]$ (see Figure 50). We label the new boundary component ∂_2' .

Note that, on the annulus Σ'' , arcs of alternating type, (o, e) or (e, o) , are exactly those which have no intersection with α . We call π_ϵ , or any sublist of consecutive entries, *alternating* if consecutive entries alternate type (so, e.g. $(1, \overline{3}, \overline{4}, 2, 5, 6)$ is of type (o, e, o, e, o, e) , and thus alternating, while $(3, 7)$ is of type (o, o) , therefore not alternating, and thus cannot be a pair of consecutive entries in any alternating word).

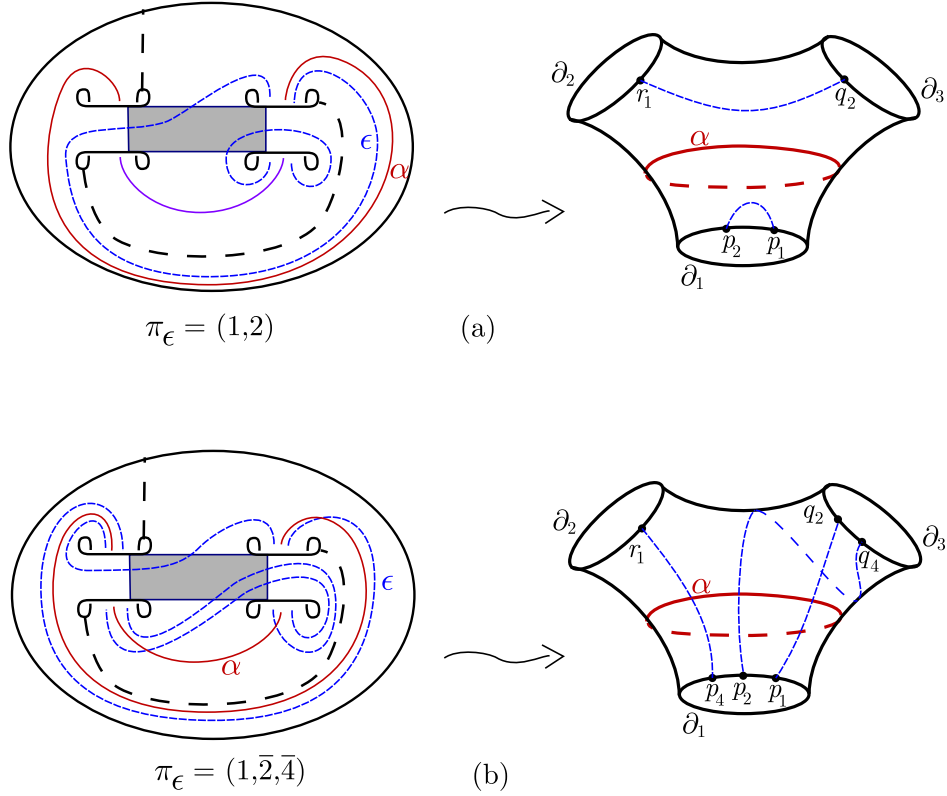


FIGURE 49. (a) A nested, balanced curve ϵ in Σ , and the result of cutting Σ as in Lemma 5.1. As demonstrated in the Lemma, such ϵ cannot intersect α . Note that each arc $\epsilon \cap \Sigma$ is paired. (b) A curve ϵ which is neither nested nor balanced. Only the arc $[p_1, q_2]$ is paired.

There are two possibilities. We have also included a detailed Example 5.2 which may help the reader keep track of notation through the following.

- (1) $m \equiv 0 \pmod{4}$

In this case, any paired arc of form $[p, p]$ would disconnect Σ'' such that one connected component has an odd number of points, a contradiction, so there is some paired arc with endpoints on ∂_2' . Each such arc disconnects a disc D with $m/2 - 2$ points, containing no pairable indices, and thus no paired arcs. Observe now that any arc in D of form $[r, r]$ or $[q, q]$ corresponds to a bigon bounded by α and one of the $\bar{\gamma}_i$, thus is disallowed by our hypotheses. Each arc in D is thus of form $[q, r]$, and therefore of type (e, o) (because an arc from r_i to q_j has the opposite derived orientation from that of s_1 , thus its indices appear in π_ϵ as (\bar{i}, \bar{j}) , while an arc from q_j to r_i appears as (j, i)).

In particular, each pair of points connected by an arc in D , and each concatenation of such pairs, corresponds to an alternating sublist of consecutive entries in π_ϵ . Furthermore, as there are exactly two paired arcs in Σ' ,

the nested condition of Definition 4.9 implies that π_ϵ is, up to cyclic permutation, of form b_1, \dots, b_m , where for each $i \leq m/2$, the entries $b_i, b_{m-(i+1)}$ are paired, and the pairs b_m, b_1 and $b_{m/2}, b_{m/2+1}$ correspond to the paired arcs. We summarize this information:

$$\pi_\epsilon = b_1 \underbrace{b_2 \dots b_{\frac{m}{2}-2}}_{(\frac{m}{2}-2) \text{ entries}} b_{\frac{m}{2}} b_{\frac{m}{2}+1} \underbrace{b_{\frac{m}{2}+2} \dots b_{m-1}}_{(\frac{m}{2}-2) \text{ entries}} b_m$$

We call $b_{m-(i+1)}$ the *reflection* of b_i . There are two key observations:

- (i): The reflection of an odd entry is even, and vice versa, so the reflection of a pair of type (e, o) is again a pair of type (e, o) .
- (ii): Let A be the set of indices of points on ∂D , separated into pairs corresponding to arcs. As noted above, A contains $m/2 - 2$ points. As D contains no paired arcs, the reflection of A , denoted A' , is disjoint from A , so $b_2 \dots b_{\frac{m}{2}-1}$ and $b_{\frac{m}{2}+2} \dots b_{m-1}$ consist entirely of pairs from A and A' .

Consider then (b_2, b_3) . By observation (ii), this is a pair in either A or A' , so by observation (i) both the pair and its reflection (b_{m-2}, b_{m-1}) are of form (e, o) . Thus each of (b_1, b_2, b_3) , (b_{m-2}, b_{m-1}, b_m) is alternating. We do the same with each pair (b_i, b_{i+1}) up to $i = \frac{m}{2} - 3$, so find that π_ϵ is alternating.

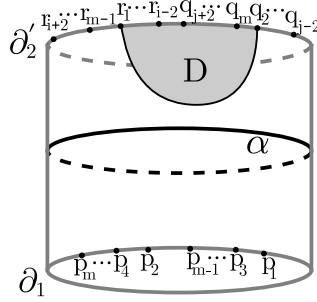


FIGURE 50. The surface Σ'' , obtained by removing an arc with endpoints $\{r_i, q_j\}$ from Σ' , and a paired arc with endpoints $\{r_1, q_2\}$. The region D separated by this arc contains no pairable indices, and so can contain no paired arcs.

- (2) $m \equiv 2 \pmod{4}$

In this case, any paired arc of form $[r, q]$ would disconnect Σ'' such that one connected component has an odd number of points, so there is some paired arc with both endpoints on ∂_1 . Each such arc disconnects a disc D with $m/2 - 1$ points, again containing no paired arcs, and now each arc on the disconnected disc corresponds to a consecutive pair in π_ϵ of form (o, e) . Again, there are exactly two paired arcs in Σ' , so π_ϵ is as in the previous case. Also, exactly one of b_1, b_m is in the pairing given by the arcs on the disc. Again, π_ϵ is alternating.

Example 5.2. We give an example of the case $m = 8$; i.e. ϵ is a nested, balanced curve such that π_ϵ has 8 entries. As noted above, there can be at most one paired arc of the form $[p, p]$, so there is one of form $[q, r]$. For

ease of notation, we assume this is $[q_8, r_7]$. Referring to Figure 48, we see that this corresponds to the pair $(8, 7)$ appearing consecutively, without bars, in π_ϵ . In particular, it is of type (e, o) . Now, this arc determines our annulus Σ'' , with points labeled as in Figure 51. Now, we are in the $m \equiv 0 \pmod{4}$ case, so any paired arc of the form $[p, p]$ will separate a disc of Σ'' with exactly 3 points, so there is another paired arc of the form $[q, r]$, say $[r_3, q_4]$ (Figure 51(a)). Again referring to Figure 48, we see that this corresponds to the pair $(\bar{3}, \bar{4})$ appearing consecutively in π_ϵ , so again of type (e, o) . Now, there can be no more nested pairs, so π_ϵ , up to cyclic permutation, is given by $(7, -, -, \bar{3}, \bar{4}, -, -, 8)$ (so is of type $(o, -, -, e, o, -, -, e)$). For the remaining entries, note that $[r_3, q_4]$ cuts a disc containing either r_1 and q_6 , or r_5 and q_2 - suppose the latter, so there is an arc $[q_2, r_5]$, again of type (e, o) . This arc corresponds to $(2, 5)$, which we insert into one of the blank pairs, say the first, to get $(7, 2, 5, \bar{3}, \bar{4}, -, -, 8)$. The remaining entries are therefore the reflection of $(2, 5)$, namely, $(6, 1)$. The corresponding ϵ (on Σ'') is illustrated in Figure 51(b). As expected, the result is alternating, and so has no intersection with α . Also, of course, this is independent of the assumptions made throughout the construction.

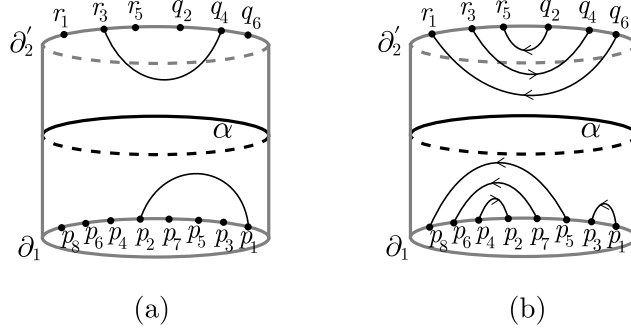


FIGURE 51. (a) A paired arc of form (p, p) separates an odd number of points, while a paired arc of form (r, q) separates an even number of points which cannot be paired. (b) The curve ϵ on Σ'' .

The curve ϵ is thus comprised of alternating strands, and so we have $\epsilon \cap \alpha = \emptyset$. □

We bring all of this together with:

Theorem 5.3. *The monodromy of the open book decomposition (Σ, φ) of $(\#^2(S^1 \times S^2), \xi_{st})$ shown in Figure 46, where ξ_{st} is the unique Stein-fillable structure, has no factorization into positive Dehn twists.*

Proof. Suppose that φ is positive, so $\tau_\alpha^{-1} \tau_{\delta_1} \tau_{\delta_2} \tau_{\beta_1} \tau_{\beta_2} = \tau_{\alpha_n} \cdots \tau_{\alpha_1}$. Then $\varphi' := \tau_{\delta_1} \tau_{\delta_2} \tau_{\beta_1} \tau_{\beta_2} = \tau_\alpha \tau_{\alpha_n} \cdots \tau_{\alpha_1}$; i.e. $\alpha \in p.e.(\varphi')$. Then, by Lemma 5.1, each α_i has trivial intersection with α . But then α must be an element of the step-down (Definition 2.3) $\mathcal{C}_{\tau_\alpha \tau_{\alpha_n} \cdots \tau_{\alpha_1}(\gamma)} = \mathcal{C}_{\varphi'}$ for any properly embedded arc γ which intersects α . The choice of γ shown in Figure 52 then gives a contradiction. □

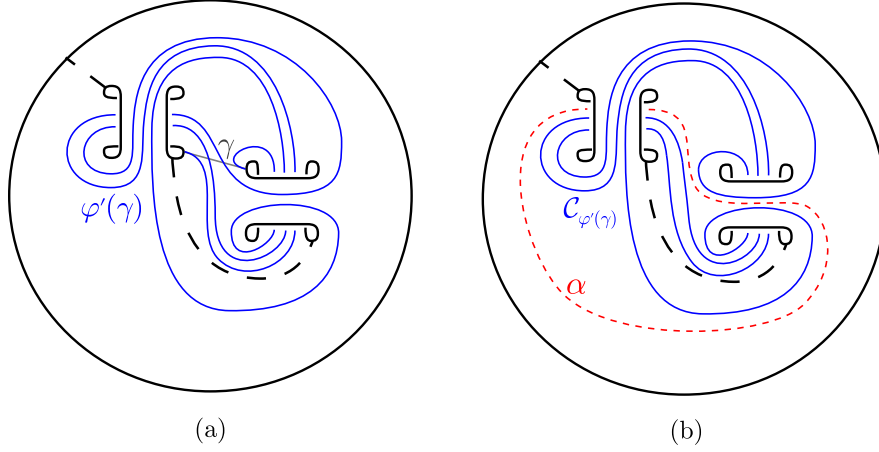


FIGURE 52. (a) The arc γ , and its image $\varphi'(\gamma)$. (b) The stepdown $\mathcal{C}_{\varphi'(\gamma)}$, and the curve α ; clearly $\alpha \notin \mathcal{C}_{\varphi'(\gamma)}$

5.3. Further examples. We conclude with some observations allowing immediate generalizations of Theorem 5.3.

Observation 5.4. Let $\psi \in \Gamma_{\Sigma_{2,1}}$ have a factorization $\psi' \circ \varphi'$, where ψ' is positive, and φ' as in the previous subsection. Then $\psi \circ \tau_{\alpha}^{-1} = \psi' \circ \varphi' \circ \tau_{\alpha}^{-1}$, and so, following the notation of Figure 45, the open books $(\Sigma_{2,1}, \psi \circ \tau_{\alpha}^{-1})$ and $(\Sigma_{2,2}, \psi' \circ \tau_{\epsilon_1} \tau_{\epsilon_2} \tau_{s'})$ are stabilization-equivalent, and in particular each support a Stein-fillable contact structure.

Observation 5.5. Let $\psi \in \Gamma_{\Sigma_{2,1}}$ be such that (ψ, D) is flat and parallel (where D is as in Figure 48), and $\alpha \notin \mathcal{C}_{\psi(\gamma)}$ (where γ is as in Figure 52). Then the proof of Theorem 5.3 holds for φ' replaced by ψ ; i.e. the monodromy $\psi \circ \tau_{\alpha}^{-1}$ has no positive factorization.

For example, $\psi := \tau_{\delta_1}^{e_1} \tau_{\delta_2}^{e_2} \tau_{\beta_1}^{e_3} \tau_{\beta_2}^{e_4}$ clearly satisfies these conditions for any positive integers e_i , so that the resulting open book decomposition $(\Sigma_{2,1}, \tau_{\alpha}^{-1} \circ \psi)$ is stabilization-equivalent to $(\Sigma_{2,2}, \tau_{\delta_1}^{e_1-1} \tau_{\delta_2}^{e_2-1} \tau_{\epsilon_1} \tau_{\epsilon_2} \tau_{s'} \tau_{\beta_1}^{e_3-1} \tau_{\beta_2}^{e_4-1})$, thus supports a Stein-fillable structure, yet its monodromy has no positive factorization. As a simple example, for the case $e_1 = e_2 = e_3 = 1$, we obtain an open book decomposition of $(S^1 \times S^2) \# L(e_4 - 1, e_4 - 2)$ for each positive e_4 (Figure 53).

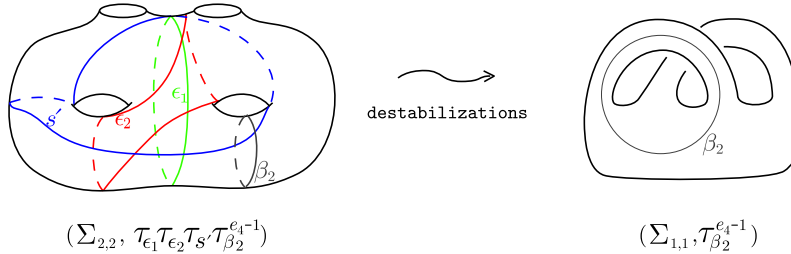


FIGURE 53. $(\Sigma_{2,2}, \tau_{\epsilon_1} \tau_{\epsilon_2} \tau_{s'} \tau_{\beta_2}^{e_4-1}) = ((S^1 \times S^2) \# L(e_4 - 1, e_4 - 2), \xi_{st})$

REFERENCES

- [BEV] K. Baker, J. B. Etnyre, and J. Van Horn-Morris, *in preparation*
- [CH] V. Colin, K. Honda, *Reeb vector fields and open book decompositions*, 2008. arXiv:0809.5088
- [EO] J. B. Etnyre and B. Ozbagci, *Invariants of contact structures from open books*, Trans. Amer. Math. Soc. 360 (2008), no. 6, 3133–3151. arXiv:math/0605441v1
- [E1] J. B. Etnyre, *Planar open book decompositions and contact structures*, IMRN **79** (2004), 4255–4267. arXiv:math/0404267v3
- [Gi] E. Giroux, *Géométrie de contact: de la dimension trois vers les dimensions supérieures*, Proceedings of the International Congress of Mathematicians (Beijing 2002), Vol. II, 405–414. arXiv:math/0305129v1
- [HKM] K. Honda, W. Kazez and G. Matic, *Right-veering diffeomorphisms of compact surfaces with boundary I*, Invent. Math. 169 (2007), no. 2, 427–449. arXiv:math/0510639v1
- [LP] A. Loi, R. Piergallini, *Compact Stein surfaces with boundary as branched covers of B^4* , Invent. Math. 143 (2001), 325348. arXiv:math/0002042v1
- [TW] W. Thurston and H. Winkelnkemper, *On the existence of contact forms*, Proc. Amer. Math. Soc. **52** (1975), 345–347.

